Biosensors and Bioelectronics 156 (2020) 112033

Contents lists available at ScienceDirect

Biosensors and Bioelectronics

journal homepage: http://www.elsevier.com/locate/bios

Carbon black as an outstanding and affordable nanomaterial for electrochemical (bio)sensor design

Fabiana Arduini [a,b,*], Stefano Cinti [c], Vincenzo Mazzaracchio [a], Viviana Scognamiglio [d], Aziz Amine [e], Danila Moscone [a]

[a] University of Rome "Tor Vergata", Department of Chemical Science and Technologies, Via della Ricerca Scientifica, 00133, Rome, Italy
[b] SENSE4MED via Renato Rascel 30, 00128, Rome, Italy
[c] University of Naples Federico II, Department of Pharmacy, Naples, Italy
[d] Institute of Crystallography, Department of Chemical Sciences and Materials Technologies, Via Salaria Km 29.3, 00015, Monterotondo Scalo, Rome, Italy
[e] Faculty of Sciences and Techniques, Hassan II University of Casablanca, Morocco

ARTICLE INFO

Keywords:
Carbon-based nanomaterials
Enzymatic biosensors
Immunosensors
DNA sensors
Paper-based biosensors

ABSTRACT

Advances in cutting-edge technologies including nanotechnology, microfluidics, electronic engineering, and material science have boosted a new era in the design of robust and sensitive biosensors. In recent years, carbon black has been re-discovered in the design of electrochemical (bio)sensors thanks to its interesting electroanalytical properties, absence of treatment requirement, cost-effectiveness (c.a. 1 €/Kg), and easiness in the preparation of stable dispersions. Herein, we present an overview of the literature on carbon black-based electrochemical (bio)sensors, highlighting current trends and possible challenges to this rapidly developing area, with a special focus on the fabrication of carbon black-based electrodes in the realisation of sensors and biosensors (e.g. enzymatic, immunosensors, and DNA-based).

1. Introduction

Since the discovery of carbon nanotubes by Iijima in 1991 (Iijima, 1991), carbon-based nanomaterials have radically changed the vision of research in several branches of science, including electrochemistry. The huge impact of nanomaterials in electroanalysis has been well documented by Escarpa (2012), he asserted that electroanalysis is undergoing a true Renaissance thanks to recent advances in several fields, such as nanotechnology. Starting from carbon nanotubes through boron-doped, graphene has recently gained momentum (Geim and Novoselov, 2010; Alwarappan et al., 2009, 2010, 2012a, 2012b; Kesavan et al., 2019; Shu et al., 2019a; Sukumaran et al., 2017; Valappil et al., 2015; Vineesh et al., 2015; Zeng et al., 2018; Zhou et al., 2018). However, recently an old and cost-effective material called carbon black (CB) has been re-discovered. CB exhibits excellent electrical conductivity, dispersible in solvents, possibility of facile functionalisation, and possesses numerous defect sites and fast electron transfer kinetics (Arduini et al., 2010a, 2010b, 2015a; Vicentini et al., 2015; Cinti et al., 2015; Mazzaracchio et al., 2019). Moreover, CB is a low-cost nanomaterial (c.a. 1 €/Kg), which further advances its use in the development of cheap electrochemical devices.

CB displays specific properties including high surface area, sphere diameter of nm size, I_D/I_G ratio higher than 0.9, and valuable heterogeneous rate constants (Table 1). The largest application of CB in the electrochemical field, until a few years ago, was in the design of sensors for analyte detection in gaseous phases, for fuel cell and lithium and sodium batteries. (Alcantara et al., 2001; Dominko et al., 2003; Hopkin and Lewis, 2001; Martinez-Alvarez and Miranda-Hernandez, 2008), while only a few CB-based electrochemical sensors had been reported up to 2009 for analyte detection in solution. As far back as 1985, Liberti et al. (1985) developed an electrochemical sensor combined with a HPLC analytical system, for the detection of phenolic compounds based on polyethylene and graphitized CB. In 2005, Razumiene et al. (2005) reported the first biosensor for reagentless determination of ethanol and glucose by exploiting this nanomaterial to create a direct electron transfer between quinohemoprotein alcohol dehydrogenase or pyrroloquinoline quinone-dependent glucose dehydrogenase.

Since 2007, CB has begun to be recognised as a reliable nanomaterial for the design of electrochemical sensors (Hocevar and Ogorevc, 2007), and an increasing number of (bio)sensing configurations have been proposed which exploit CB's multifunctional features, as highlighted by relevant research groups (Lo et al., 2012; Wong et al., 2012; Vicentini et al., 2015). For instance, in 2010 our group demonstrated the suitability of CB to develop both carbon-paste (Arduini et al., 2010a) and

* Corresponding author. University of Rome "Tor Vergata", Department of Chemical Science and Technologies, Via della Ricerca Scientifica, 00133, Rome, Italy.
E-mail address: fabiana.arduini@uniroma2.it (F. Arduini).

https://doi.org/10.1016/j.bios.2020.112033
Received 25 November 2019; Received in revised form 6 January 2020; Accepted 15 January 2020
Available online 29 January 2020
0956-5663/

screen-printed electrodes (Arduini et al., 2010b). The outstanding features of this *underestimated* nanomaterial were also demonstrated when compared with the most commonly used carbon nanotubes and graphene. In 2012 the Compton group demonstrated the effectiveness of commercial Monarch® CB samples (M 1100), compared to the more specialised multi-walled carbon nanotubes to produce a carbon paste sensor for nicotine detection. Lower background currents associated with larger Faradaic currents with higher signal/noise ratio was observed in the case of a CB-based paste electrode, highlighting "*the potential improvement involved in the (largely unexplored) direct application of nano-carbon in electrode surface modification*" (Lo et al., 2012). The Pumera group reported a comparison between CB (Grade 5358R) and thermally reduced graphene oxide, and demonstrated that thermally reduced graphene oxide held no advantage over CB for both inner-sphere (e.g. $[Fe(CN)_6]^{4-/3-}$) and outer-sphere (e.g. $[Ru(NH_3)_6]^{2+/3+}$) redox probes. The authors stated that "*for electrochemical sensing purposes we suggest CB as an electrode material in lieu of thermally reduced graphene oxide due to its low cost and time saving since it can be used "as is" from commercial suppliers, with little or no loss in electrochemical performance*" (Wong et al., 2012). In 2015, Banks and Fatibello-Filho groups studied three different CB samples to modify glassy carbon electrodes describing the "*significant improvements in the electrochemical performance (excellent sensitivity, faster heterogeneous electron transfer rate (HET)) over that of a bare glassy-carbon and edge-plane pyrolytic graphite electrode and thus suggest that there are substantial advantages of using CB as modifier*" (Vicentini et al., 2015). Thanks to these initial efforts, CB's outstanding electrochemical performances have increased the use of this cost-effective and sustainable nanomaterial in the construction of electrochemical (bio)sensors. Fig. 1, demonstrates the increasing role of this carbon-based material in the design of electrochemical (bio)sensors.

In the next sections, a glance at CB-based electrochemical (bio) sensing configurations is reported, with a special focus on the use of CB for the design of both sensors and biosensors (e.g. enzymatic, immunosensors, and DNA-based), as well as paper-based (bio)sensors.

2. Fabrication of CB-based electrodes

According to definite analytical requirements and economic opportunities, different approaches have been adopted for the manufacturing and modification of electrochemical sensors, from the oldest carbon paste to glassy carbon and printed electrodes. Among nanomaterials, CB has shown high potential in the customization of all these types of electrodes (Fig. 2), thanks to its fascinating electrochemical features, combined with cost-effectiveness.

2.1. Carbon paste electrodes

CB-based paste electrodes have been produced in a variety of configurations by exploiting the versatility of carbon paste and CB nanomaterial. Hočevar and Ogorevc created CB-paste micro-electrodes using Printex XE2 CB and mineral oil, packing this paste into pulled micro-meter glass capillaries by using a newly developed piston-driven system (Hocevar and Ogorevc, 2007). A solid CB-based paste was prepared by hand, mixing CB and solid paraffin, liquefied by heating to around 45 °C before mixing with CB. 50% of solid paraffin was required in order to obtain a stable CB-paste paste, while only 25% of solid paraffin was sufficient for graphite paste electrodes, being CB characterised by high surface area and thus requiring high amounts of binder (Malha et al., 2013). Another approach for CB-based paste production relies on the construction of a carbon concentrate of technical polyethylene in the form of black granules, made up of 30% CB N220 and 70% thermally stabilized polyethylene. This material was then melted to fill the electrode body (the internal diameter of the shell 3.9 mm with an internal stainless steel contact), this was further modified with gold nanoparticles by electrodeposition of $AuCl_4^-$ and utilized for iron detection (Zakharova et al., 2012).

Malha et al. (2016) investigated several CB nanomaterials using CB N110, N220, N375, N772 all mixed with 50% (w/w) liquid or solid paraffin, demonstrating that the use of solid binders in CB paste electrodes allows for an easier renewal of the working electrode surface. The Compton group prepared different CB-based carbon paste electrodes by hand pasting CB powder with mineral oil, paraffin oil or [C4mpyrr][NTf2]. In particular, two CB-based paste electrodes were fabricated using the following ratio: graphite/CB/[C4mpyrr][NTf2]/mineral oil (12/37/14/17) and CB/mineral oil (55/45) to test compounds characterised by reversible behaviour such as $Ru(NH_3)_6^{3+}$, $FcCH_2OH$ and acetaminophen (Lowinsohn et al., 2013). This study demonstrated a similar electrochemical performance between graphite and CB; however, CB can be considered a valid alternative to graphite powder for its affordability (ca. 25 times cheaper than graphite). In the case of species characterised by irreversible behaviour such as nitrite, a shift of ca. 150–200 mV toward lower potential was observed, demonstrating that the benefit of CB is not just confined to the cost, but it also establishes an improvement to the electrochemical properties (Malha et al., 2013).

2.2. Glassy carbon electrodes

Among the diverse electrodes used in electrochemistry, glassy carbon is the main electrode used to test and characterise new nanomaterials. To deliver a nanomodified glassy carbon electrode, the drop-casting procedure is the principal approach for a fast and reliable modification of the

Table 1

Carbon Black	Particle diameter (nm)	Surface Area (BET) (m^2/g)	I_D/I_G	k^0 (cm/s)	References
BP4750	25 (a)		3.65 (a)	$5.74\ 10^{-3}$ (a)	a) Vicentini et al., 2015
ECP-600JD	34 (b)	1270 (b)			b) Lee et al., 2012
E2000	25 (a)		2.36 (a)	$6.23\ 10^{-4}$ (a)	c) Mazzaracchio et al., 2019
HP 160			1.28 (c)	$5.4\ 10^{-3}$ (c)	d) Lo et al., 2012
HS20			1.32 (c)	$1.2\ 10^{-3}$ (c)	e) Lowinsohn et al., 2013
M 1100	14 (d)				f)https://www.mt.com/ch/it/home/supportive_content/matchar_apps/MatChar_HB457.html
M 430	25-37 (e)				
MT N990		9 (f)	1.19 (c)		
N115		142(g)	1.33 (c)	$6.3\ 10^{-3}$ (c)	g) Donnet et al., 2002
N220	17.95-32.5 (h)	120 (h)	0.96 (h)	$1.59\ 10^{-2}$ (h)	h) Arduini et al., 2010a
N375	36 (i)	105 (i)	1.27 (c)	$3\ 10^{-3}$ (c)	i) Malha et al., 2016
N660		35 (l)	1.2 (c)	$2.6\ 10^{-3}$ (c)	l)https://www.makrochem.com/specs/n660.pdf
N772	124 (i)	30 (i)			
Printex XE 2	30 (m)	950 (n)		$8.1\ 10^{-3}$ (n)	m) Hocevar et al., 2007
5358R	29 (p)		0.91 (p)	$1.7\ 10^{-3}$ (p)	n) Svegl et al., 2008
PL6		150 (q)	1.41 (c)	$4.8\ 10^{-3}$ (c)	p) Wong et al., 2012
Super P		62 (r)	1.41 (c)	$2.2\ 10^{-3}$ (c)	q) Al-Hartomy et al., 2012
XE2B		1000 (s)	1.57 (c)	$4.3\ 10^{-3}$ (c)	r) www.matweb.com
VXC72R	25 (a)	254 (t)	2.64 (a)	$9.26\ 10^{-2}$ (a)	s) Al-Hartomy et al., 2011
					t) Yang et al., 2017

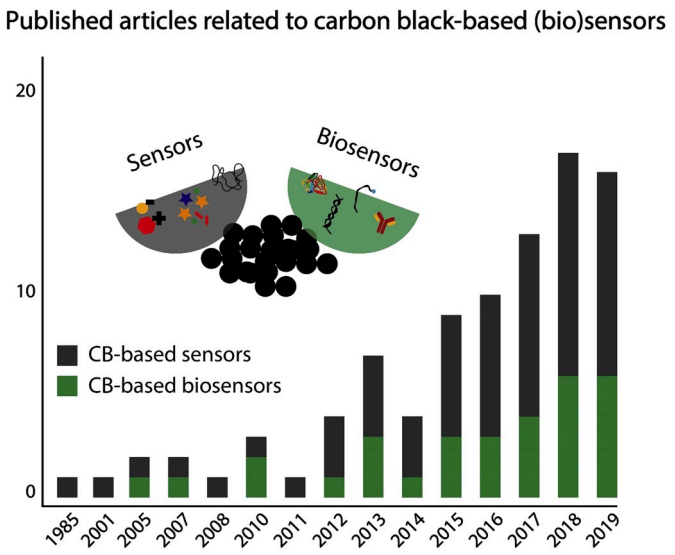

Fig. 1. Published articles related to electrochemical (bio)sensors using CB as nanomaterials and their distribution among sensors and biosensors.

working electrode surface. Therefore, a stable dispersion is required to provide a highly reproducible sensor, and to avoid any non-homogenous coverage of the working electrode surface, with a consequent irreproducible immobilisation of bio-components during a biosensor construction.

One of the main features of CB is its ability to easily produce stable dispersions, usually at a concentration of 1 mg/mL in a variety of solvents such as ethanol, acetonitrile, a mixture of dimethylformamide-water in ratio 1:1 (v/v) (Mazzaracchio et al., 2019), chitosan (Talarico et al., 2016), cetyltrimethylammonium bromide (Svegl et al., 2008) or dihexadecylphosphate water solution (Silva et al., 2017).

For instance, Vicentini et al. evaluated the electrochemical response of glassy carbon electrodes modified with a few μL of CB-dispersions, prepared as follows: i) 1.0 mg CB in 1.0 mL of ultrapure water; ii) 1.0 mg of CB and 1.0 mg of dihexadecylphosphate in 1.0 mL of ultrapure water; and iii) 1.0 mg of CB in 1.0 mL chitosan solution (1.0% w/w), all dispersions were sonicated for 30 min. To select the best dispersion, potassium ferrocyanide was selected as the electrochemical probe and cyclic voltammetry as the electrochemical technique, with an evaluation of peak-to-peak separation and peak intensity. The highest current with improved electrochemical reversibility (i.e. close peak-to-peak separations) was obtained with chitosan based-dispersion, because no adherent and stable films were found without chitosan (Vicentini et al., 2015). In fact, CB dispersion with water requires polymers such as chitosan, or additional organic solvents such as dimethylformamide (Arduini et al., 2012).

In different conditions, organic solvents, including acetonitrile, have delivered stable dispersions (Arduini et al., 2010b). Indeed, CB dispersion prepared in ethanol, acetonitrile, or a mixture of dimethylformamide: water remained stable for several months (Arduini et al., 2012), and avoided multiple additional sonication steps. It is noteworthy that CB N330 can be converted into carbon nanosheets, a few nanometer's thick, after ultrasound irradiation at room temperature and atmospheric pressure under nitrogen for 44 h, causing the loss of CB's particular structure (Li et al., 2007); thus multiple steps of sonication must be avoided.

The alternative use of polymers as additional reagents can affect the

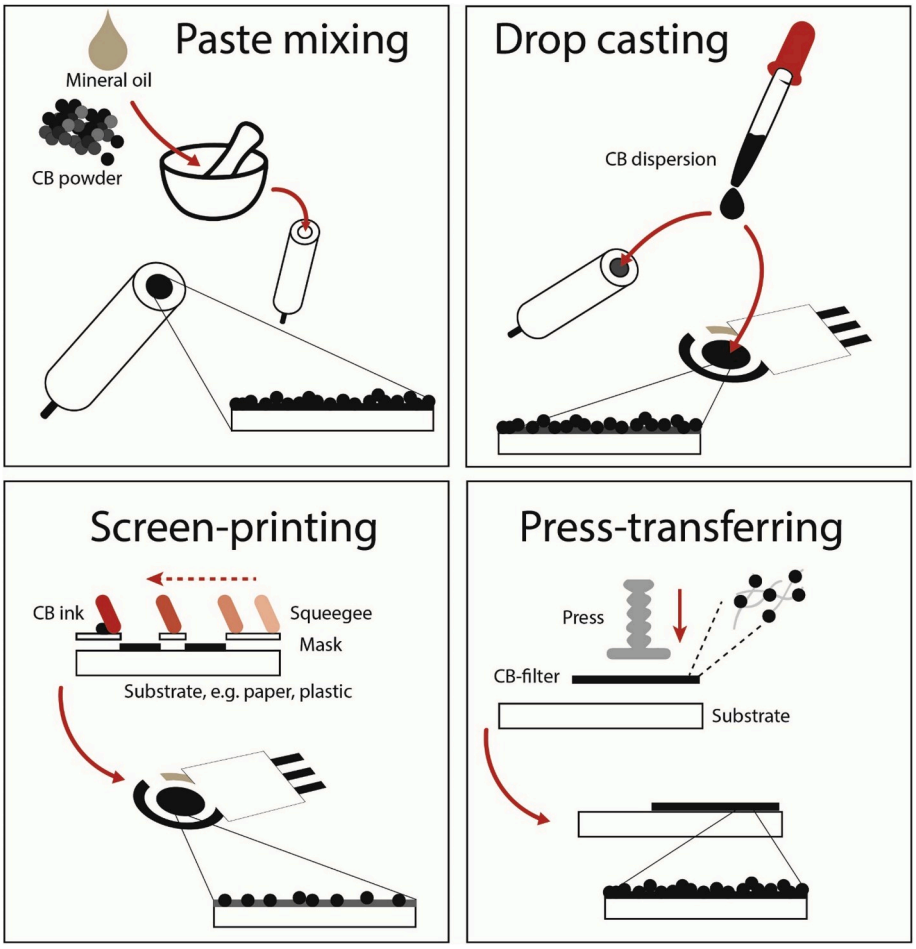

Fig. 2. Different procedures to fabricate CB-based (bio)sensors.

selectivity and sensitivity of the sensors. For instance, CB was used to modify glassy carbon electrodes by creating a CB-film of alginate cross-linked with glutaraldehyde. In this case, alginate resulted in being an optimal polysaccharide for working electrode surface modification in comparison with cellulose, pectin, starch, and chitosan, and showed a stronger interaction with the target analyte (i.e. paraquat) and thus an improved selectivity and sensitivity of the sensor (Pacheco et al., 2019).

2.3. Screen-printed electrodes

The versatility of screen-printed electrodes is not confined to their capability of being integrated in microfluidic systems, in the requirement of low volume samples, or in the easiness of use and miniaturisation; it also covers the modification approach (Fig. 2).

The modification of screen-printed electrodes with CB is carried out by two different processes: i) modification of the printed sensor during the electrode fabrication by adding CB to the graphite ink, delivering CB-bulk modified electrodes; or ii) modification of the printed sensor by drop-casting using a CB-dispersion, providing a "film" modified sensor.

The bulk approach allows for the production of the CB-sensor during the fabrication, thus permitting a single step production process; however, it requires a total homogeneity of the inks to obtain a high level of repeatability (RSD% lower than 10%). In addition, the surface coverage depends on the amount of CB (w/w) added to the ink; amounts higher than 10% cannot be used because viscosity increases, affecting the correct deposition of the inks. With an increase in the CB amount in the inks, a higher coverage of CB has been observed. However, using ferricyanide as electrochemical probe and cyclic voltammetry as electrochemical technique, the lower peak to peak separation associated to the higher intensity peak current has been observed using SPEs modified with CB by drop-casting (Arduini et al., 2012). Besides the conventional electrodes, printing technology has aided the creation of new sensors by making use of smart supports, and CB has demonstrated its capability of improving their electrochemical performance. This is the case of sensors printed on alternative substrates as filter, office, paper towel, waxed paper, and Parafilm M® (Heathrow Scientific, Vernon Hills, IL, USA) (Cinti et al., 2017a, 2018a, 2019; Colozza et al., 2019) or paper employed in printed electronics (i.e. p e:smart) (Cinti et al., 2018b). For instance, CB was successfully used to modify electrodes that had been screen-printed on paper used in printed electronics field with a drop-casting approach. This provides lower peak-to-peak separation, higher current intensity, and lower resistance of charge transfer.

2.4. Microfluidic press-transferred

If our group has been the pioneer in the fabrication, characterisation, and application of CB-based printed (bio)sensors, Escarpa and Compagnone groups have recently established the possibility of transferring CB to non-conductive supports for the development of microfluidic devices. Tapping into press-transfer technology has allowed for the design and control of the electrical properties of conductive CB films, and produced customised films with ohmic and tunnelling conductivity tailored for electrochemical detection (Della Pelle et al., 2017). In detail, a dispersion of CB N220 in 1,2-dichloroethane was vacuum filtered onto a Teflon filter, obtaining a CB "wire", which was successively press-transferred onto a poly(methyl methacrylate) substrate. This approach enabled the smart construction of a working electrode to detect phenols in olive oil extracts (Della Pelle et al., 2017) or pesticides in environmental samples (Della Pelle et al., 2016).

2.5. 3D-printed

Among the different printing techniques including screen- and ink-jet printing, 3D printing is an emerging technology capable of producing three-dimensional objects with customized shapes and dimensions, using a cost-effective and fast manufacturing process. Diverse components of the electrochemical set-up have been fabricated using 3D printing technology, such as a holder to contain a paper-based electrode (Scordo et al., 2018) or a flow cell for electrochemical measures (Snowden et al., 2010).

In this rapidly growing area, in 2019, for the first time, Banks group reported a three-electrode system created with 3D-printing technology using CB as one of the main components (Richter et al., 2019). The working, counter and pseudo-reference electrodes were produced by using a conductive fused filament made up of a mixture of CB and polylactic acid. To realise the reference electrode, the CB-based electrode was covered with silver ink to deliver an Ag-pseudroreference electrode, while in the case of the working electrode, an electrochemical activation in sodium hydroxide was required to enhance any electrochemical behaviour. The analytical performances were investigated using dopamine as model compound by square wave voltammetry, obtaining a limit of detection equal to 0.1 μM with a linear range up to 250 μM.

3. CB-based biosensors

CB has been widely exploited in the design of biosensors in joint conjunction with several biological recognition elements including enzymes, DNA, and antibodies (Table 2). This perfect combination relies on its properties: i) it enlarges the loading surface area for bioreceptor immobilisation, ii) it increases electrochemical behaviour and thus sensitivity; and iii) it is compatible with the exploited biological receptors.

3.1. Enzymatic biosensors

The main potential of the combination of enzymes with CB relies on the outstanding advantages this nanomaterial has in enhancing biosensor sensitivity. Indeed, CB is able to augment both conductivity and enzyme loading areas, thus resulting in enhanced signals and consequently in higher sensitivity. Moreover, some examples demonstrated the CB as a compatible substrate for enzymes immobilisation in the design of amperometric biosensors.

Various enzymes have been associated with CB, including tyrosinase, laccase, glucose dehydrogenase, glucose oxidase, acetylcholinesterase, butyrylcholinesterase, and alcohol dehydrogenase. Arduini et al. (2010a) combined tyrosinase with a CB paste electrode to realise a biosensor for the amperometric detection of catechol. In detail, a tyrosinase carbon paste electrode was constructed using 10% by weight of tyrosinase, 50% of graphite, and 40% of mineral oil, similar to the composition already described in literature for a tyrosinase biosensor based on carbon nanotubes. In the case of the graphite biosensor, ca. 30% of mineral oil amount is required, but CB provides, similarly to carbon nanotubes, a higher surface area compared to graphite, thus requiring a higher amount of mineral oil (Mita et al., 2007). However, despite the nanomaterial/enzyme/oil composition being similar to those of carbon nanotubes, the authors described an enhanced sensitivity (625 nA/μM) and lower detection limit (0.008 μM) in comparison with the carbon nanotube-based biosensor. The enzymatic product (quinone) is reduced to hydroquinone (catechol) which is oxidised again as substrate by tyrosinase. This led to an enzymatic amplification cycle, whose efficiency depended on the electroactivity of quinone and on the close proximity of the enzyme and carbon material. Therefore, CB was able to load a higher amount of enzyme thanks to its high surface area and its close proximity to the bioreceptor, to obtain a higher sensitivity of the system.

A glassy carbon electrode modified with functionalised CB was also described in order to enhance the electrochemical performances of a tyrosinase biosensor for the detection of catechol in water samples (Ibáñez-Redín et al., 2018). The functionalisation of CB entailed the oxidation with nitric and sulphuric acids 1:1 (v/v) mixture for 30 min at 25 °C, allowing for an increase of material wettability due to augmented oxygenated functional groups. The biosensor was constructed by modifying the electrode with CB dispersion in a dihexadecylphosphate-based water solution, followed by the tyrosinase enzyme immobilisation using bovine serum albumin and

glutaraldehyde. This device showed a sensitivity of 539 mA mol^{-1} L and a limit of detection of 8.7 × 10^{-8} mol L^{-1} (Fig. 3A). Nadifiyine et al. (2013) developed a biosensor based on tyrosinase and CB paste electrode, demonstrating a reduced noise compared to traditional graphite paste enzymatic electrodes, with an increased sensitivity, allowing for a detection limit of 6 nmol L^{-1} for catechol. The suitability of this biosensor was tested for phenol quantification in olive oil, and proved a good statistical correlation between the results obtained with the proposed CB-based biosensor and the reference method (i.e. *Folin-Ciocalteu* spectrophotometric method).

Laccase has also been selected as polyphenol oxidase for CB-based biosensor design. As an example, a laccase-based biosensor was realised using a thionine/CB-modified screen-printed electrode for the detection of bisphenol A (Portaccio et al., 2013). Here, the enzyme was entrapped onto the electrode surface by a neutralised aqueous solution of Nafion while CB was exploited to absorb thionine as electrochemical mediator, avoiding its leakage. Under optimized conditions in terms of enzyme loading, pH and applied potential, a linear concentration range up to 50 μM was described, with a limit of detection of 0.2 μM. This biosensor was also tested in tomato juice samples contained in metallic cans where bisphenol A can be released due to the epoxy resin coating, with a satisfactory recovery value between 92% and 120%.

A CB modified laccase-biosensor was also realised for the detection of hydroquinone as a typical model of phenolic compounds. CB paste electrodes were prepared by mixing 30% w/w CB and 70% w/w mineral oil. This configuration showed a stability over 5-months. The laccase enzyme was adsorbed onto a film made with botryosphaeran (from Botryosphaeria rhodian) and gold nanoparticles. Square wave voltammetry was used to detect hydroquinone within the range 2.00–56.5 μM with a calculated detection limit of 0.474 μM. The presence of other phenol-like compounds such as epinephrine, dopamine, guaiacol and catechol, although producing a response, did not significantly interfere with the current signal corresponding to hydroquinone. The laccase biosensor was applied towards many matrices such as dermatological cream, samples from biological (human urine) and environmental niches (river water), and obtained excellent recovery results with values close to 100% (Mattos et al., 2019).

Among enzymes suitable for enzymatic substrate detection, glucose oxidase fits impeccably with CB in the design of sensitive electrochemical biosensors. The preparation of a carbon composite electrode based on a mixture of CB, poly(ethylene-*co*-vinyl acetate), and Prussian blue was described for the immobilisation of glucose oxidase in the design of an amperometric biosensing system for glucose detection in tears with a detection limit of 7.8 μM within a linear range up to 6.95 × 10^{-4} M (Calegari et al., 2017). In detail, CB was used for potentiodynamic deposition of a Prussian blue film, allowing for the detection of the glucose oxidase by-product hydrogen peroxide, at an applied potential of −400 mV. Artificial tears spiked with glucose were also analysed with recovery values from 96.5 to 105%. CB combined with mesoporous carbon has been used to deliver an organophosphorus hydrolase biosensor for pesticide detection. The low detection limit of paraoxon (36 ppb) has been achieved by exploiting the high sensitivity of this nanocomposite towards p-nitrophenol, which is the enzymatic by-product of the organophosphorus hydrolase. The effectiveness of this configuration was also demonstrated when compared to a carbon nanotube-modified electrode, because CB combined with mesoporous carbon is capable of promoting the electron transfer of enzymatically generated phenolic compounds better than only carbon nanotubes (Lee et al., 2010).

An alternative strategy using enzymes as biocomponent relies on the detection of enzymatic inhibitors. Cholinesterase enzyme is undoubtedly the leading actor in inhibitive biosensors, thanks to its high enzymatic reaction rate as well as sensitivity towards reversible and irreversible inhibitors (Amine et al., 2016). Cholinesterase biosensors have been successfully developed in conjunction with CB, showing increased sensitivity and minimised fouling problem from the enzymatic by-product thiocholine, probably due to the high number of defect sites. For instance, Arduini et al. (2015b) designed a printed electrode modified by drop-casting with CB to further immobilise butyrylcholinesterase enzyme by cross-linking through glutaraldehyde, Nafion, and bovine serum albumin. The antifouling property of CB was demonstrated in the detection of thiocholine at the oxidative potential; indeed, six successive analyses of the enzymatic substrate butyrylthiocholine gave RSD% equal to 3.9, demonstrating the stability of the signal without fouling effect. This biosensor measured paraoxon with a detection limit of 5 μg L^{-1}, whose inhibition was linearly described up to 30 μg L^{-1}. The suitability of this biosensor was also highlighted for the analysis of water samples fortified with 50 μg L^{-1} of paraoxon, a level lower than the Italian legal limit of 100 μg L^{-1} for surface waste waters (DL 152/2006), obtaining a recovery value of 96 ± 2%. Moreover, it showed a very high stability up to 78 days when stored at RT in dry conditions, with RSD% not higher than 6% for all the inhibition analyses performed. Finally, its applicability in complex matrices was also largely demonstrated without sophisticated sample pre-treatment and interference problems, thanks to the adopted "medium exchange method" (Arduini and Amine, 2013). This method consisted of three steps. In the first step, the enzymatic activity was measured in buffer solution in the presence of the enzymatic substrate. In the second step, the biosensor was put in contact with the sample which had been contaminated with insecticides for a selected time, followed by washes with distilled water. In the last step, the enzymatic residual activity was determined in a new buffer aliquot in the presence of the only enzymatic substrate. This approach avoided electrochemical interferences (e.g. ascorbic acid and phenolic compounds), because the enzymatic activity was quantified in the absence of any electroactive interfering species as well as reversible inhibitors, which are eliminated during the washing step (Amine et al., 2016). The suitability of this biosensor was highlighted not only for environmental analysis, but also in the agrifood sector to detect pesticides in olive oil (Arduini et al., 2017). In particular, olive oil samples treated with the QuEChERS method to extract pesticides from the whole fatty matrix were analysed for the presence of paraoxon by exploiting butyrylcholinesterase immobilised on CB modified screen-printed electrodes, with a detection limit of 6 ppb. The accuracy of this biosensor was assessed with olive oil spiked with paraoxon, obtaining a satisfactory recovery value.

The same enzyme and immobilisation procedure were exploited to deliver a highly sensitive biosensor for paraoxon detection using screen-printed electrodes modified with a nanocomposite dispersion made up of CB and cobalt phthalocyanine. In this case, CB was used to load cobalt phthalocyanine to obtain a stable dispersion, suitable for the production of highly reproducible drop-cast modified sensors, allowing for paraoxon quantification with a detection limit equal to 18 nM (Cinti et al., 2016a).

A different immobilisation procedure was exploited for fabrication of an acetylcholinesterase-based biosensor using screen-printed electrodes modified by drop-casting, with a dispersion of CB and chitosan. In detail, a one-step drop-casting procedure allowed depositing CB, chitosan, and acetylcholinesterase on working electrode, leading to an easy and customised mass-production of this biosensor. This biosensor was tested with paraoxon, demonstrating a linearity range up to 0.5 μg L^{-1} and a low detection limit of 0.05 μg L^{-1} (calculated as 10% of inhibition). In addition, drinking water samples spiked with paraoxon have been tested with recovery values equal to 97 ± 15% (Talarico et al., 2016).

Acetylcholinesterase-based biosensors have also been designed by the Evtugyn group, coupling CB with metallic nanoparticles and macrocyclic ligands. In the first case, thiacalix[4]arene was employed for the synthesis of Ag nanoparticles, working both as a reducing and encapsulating agent, avoiding nanoparticles aggregation, and this nanocomposite was then cast on the glassy carbon electrode. Subsequently, 2 μL of the acetylcholinesterase solution was loaded onto the electrode surface without any additional reagent (Fig. 3B). This biosensor proved its capability of detecting organophosphorus and carbammic pesticides at nM-μM level in standard solution as follows: malaoxon 0.4 nM–0.2 μM, paraoxon 0.2 nM–0.2 μM, carbofuran 0.2 nM–2.0 μM, aldicarb 10 nM–0.20 μM and residual amounts of pesticides in spiked samples of peanut and grape juice (Evtugyn et al.,

Table 2

Biocomponent	Sensor	CB type, dimension and modification procedure	Biocomponent immobilisation	Electrochemical technique	Analyte	Linear range/LOD	Sample	Reference
Enzyme (Tyr)	CB/CP	N220, 19-29 nm, Enzyme:CB:oil mixed in molar ratio (10:45:45)	Entrapment	Amperometry	Catechol	0.008 μM	–	Arduini et al., 2010a
Enzyme (Tyr)	CB/DHP/GC	Vulcan XC 72R, 10-500 nm Dispersion 1 mg/ml, drop casting	Cross-linking	Amperometry	Catechol	1-20 μM/0.087 μM	Water	Ibanez-Redin et al., 2018
Enzyme (Tyr, Lac, Per)	CB/CP	N220, CB:oil mixed in molar ratio (50:50)	Cross-linking	Amperometry	Catechol	0.013-150 μM/0.006 μM (CB/CP-Tyr) 0.090-15 μM/0.030 μM (CB/CP-Lac) 0.050-21 μM/0.010 μM (CB/CP-Per)	Olive Oil	Nadifiyine et al., 2013
Enzyme (Lac)	Thionine/CB//SPE	N220, dispersion 1 mg/ml in acetonitrile, drop casting	Physical adsorption	Amperometry	BPA	0.5-50 μM/0.2 μM	Tomato Juice	Portaccio et al., 2013
Enzyme (GOx)	PB/CB/EVA Composite Electrode	N220, N220:EVA mixed in molar ratio (25:75)	Cross-linking	Amperometry	Glucose	99-695 μM/7.8 μM	Artificial Tears	Calegari et al., 2017
Enzyme (OPH)	MC/CB/GC	Carbon® ECP-600JD, 34 nm	Physical adsorption	Amperometry	Paraoxon	0.2-8 μM/0.12 μM	–	Lee et al., 2010
Enzyme (BChE)	CB/SPE	N220, 19-29 nm, dispersion 1 mg/ml in DMF:H_2O (1:1, v/v), drop casting	Cross-linking	Amperometry	Paraoxon	0.018-0.11 μM/0.018 μM	Wastewater	Arduini et al., 2015b
Enzyme (BChE)	CB/SPE	N220, dispersion 1 mg/ml in DMF:H_2O (1:1, v/v), drop casting	Cross-linking	Amperometry	Paraoxon	0.072-0.36 μM/0.022 μM	Olive Oil extract	Arduini et al., 2017
Enzyme (BChE)	CB-CoP/SPE	N220, 17.95-32.5 nm, dispersion 1 mg/ml in DMF:H_2O (1:1, v/v), drop casting	Cross-linking	Amperometry	Paraoxon	0.036-0.11 μM/0.018 μM	Wastewater	Cinti et al., 2016a
Enzyme (AChE)	CB-CS/SPE	N220, 17.95-32.5 nm, dispersion 3 mg/ml in CS (0.05% w/w), drop casting	Enzyme mixed in CB-CS dispersion	Amperometry	Paraoxon	0.00036-0.0018 μM/0.00018 μM	Drinking Water	Talarico et al., 2016
Enzyme (AChE)	AgNPs-TC/CB/GC	N220, dispersion 1 mg/ml in DMF, drop casting	Cross-linking	Amperometry	Paraoxon, Malaoxon, Carbofuran, Aldicarb	0.0002-0.2 μM/0.00005 μM (Paraoxon) 0.0004-0.2 μM/0.0001 μM (Malaoxon) 0.0002-2 μM/0.0001 μM (Carbofuran) 0.01-0.2 μM/0.01 μM (Aldicarb)	Peanut, Grape Juice	Evtugyn et al., 2014
Enzyme (AChE)	PA/CB/GC	N220, dispersion 1 mg/ml in DMF, drop casting	Cross-linking	Chronoamperometry	Paraoxon, Malaoxon, Carbofuran, Aldicarb	0.01-7 μM/0.005 μM (Paraoxon) 0.00001-1 μM/0.000004 μM (Malaoxon) 0.0001-2 μM/0.00002 μM (Carbofuran) 0.007-10 μM/0.0006 μM (Aldicarb)	Peanut, Beetroot	Shamagsumova et al., 2015
Enzyme (BChE)	Paper-based CB-PBNPs/SPE	N220, CB-PBNPs nanocomposite dispersion 1 mg/ml in DMF:H_2O (1:1, v/v), drop casting	Physical adsorption into paper network	Chronoamperometry	Paraoxon	Up to 0.09 μM/0.011 μM	Wastewater, River Water	Cinti et al., 2017c
Enzyme (BChE, AP, Tyr)		N220, CB-PBNPs nanocomposite	Physical adsorption into paper network	Chronoamperometry	Paraoxon, 2,4 D, Atrazine		River Water	Arduini et al., 2019

(*continued on next page*)

Table 2 (*continued*)

Biocomponent	Sensor	CB type, dimension and modification procedure	Biocomponent immobilisation	Electrochemical technique	Analyte	Linear range/LOD	Sample	Reference
	Origami Paper-based CB-PBNPs/SPE	dispersion 1 mg/ml in DMF:H_2O (1:1, v/v), drop casting				2- 20 ppb/2 ppb (Paraoxon) up to 600 ppb/50 ppb (2,4 D) 10-100 ppb/(Atrazine)		
Enzyme (ChOx)	Paper-based CB-PBNPs/SPE	N220, CB-PBNPs nanocomposite dispersion 1 mg/ml in DMF:H_2O (1:1, v/v), drop casting	Physical adsorption into paper network	Amperometry	Sulphur Mustard	1-4 mM/0.9 mM	–	Colozza et al., 2018
Antibody (Anti-Cardiac Myoglobin)	DDAB/CB/SPE	N220, 19-29 nm, dispersion 1 mg/ml in DMF:H_2O (1:1, v/v), drop casting	Physical adsorption	Square Wave Voltammetry	Cardiac Myoglobin	5-500 μM	Plasma	Suprun et al., 2012
Antibody (Anti-p53)	CB-CS/ITO	Super P, CB-CS composite, spin coating	Cross-linking	EIS	Protein p53	0.01-2 pg/ml/3 fg/ml	Serum	Aydin et al., 2018a
Antibody (Anti-Interleukin-8)	CB-CS-SPGMA-PVDF/ITO	Super P, CB-CS- SPGMA-PVDF composite, spin coating	Cross-linking	EIS	Interleukin-8 Biomarker	0.01-3 pg/ml/3.3 fg/ml	Serum, Saliva	Aydin et al., 2018b
Antibody (Anti-C-reactive proteine)	PS-CB composite electrode	Vulcan XC72, PS-CB ink, spin coating	Physical adsorption	Hot electron-induced electrochemiluminescence	C-reactive protein	5.3 μg/L	–	Salminen et al., 2018
DNA (ds-DNA from salmon sperm)	PA/CB/GC	Dispersion 1 mg/ml in CS (0.375% w/w), drop casting	Electropolymerization of Neutral Red in presence of DNA	Voltammetry	DNA damage by Reactive oxygen species	–	–	Kuzin et al., 2018
DNA	AuNPs/CuS-AB/GC	Acetylene Black, CuS- Acetylene Black nanocomposite dispersion, drop casting	Au–S	Differential Pulse Voltammetry	Complementary ssDNA target	0.1 pM-1 nM/0.02 pM	–	Huang et al., 2015
DNA	AuNPs/WS_2-AB/GC	Acetylene Black, WS_2-Acetylene Black nanocomposite dispersion, drop casting	Au–S	Differential Pulse Voltammetry	Complementary ssDNA target	0.001-100 pM/0.12 fM	–	Shuai et al., 2016
DNA (Anti-microRNA-125a DNA)	CB/Pencil Graphite	N220, 32 nm, dispersion 1 mg/ml in DMF or Acetonitrile, drop casting	Cross linking	EIS	MicroRNA-125a	0.001-2 μM/10 pM	Serum	Yammouri et al., 2017
DNA (Anti-microRNA-21)	AuNPs/CB/ Pencil Graphite	N220, 32 nm, dispersion 1 mg/ml in DMF, drop casting	Au–S	Differential Pulse Voltammetry	MicroRNA-21	2.9 fM -700 nM/1 fM	Serum	Yammouri et al., 2019
Molecularly imprinted polymer	aGO/CB-OMNiDIP/SPE	aGO-CB composite, drop casting		Differential pulse anodic stripping voltammetry	Dopamine, Epinephrine	Dopamine: 28 pg/mL (Water), 28 pg/mL (Serum), 61 pg/mL (Urine) and 29 pg/mL (Pharmaceutical sample) Epinephrine: 17 pg/mL (Water), 18 pg/mL (Serum), 19 pg/mL (Urine) and 20 pg/mL (Pharmaceutical sample)	Water, Serum, Urine, Pharmaceutical samples	Fatma et al., 2019

AChE = Acetylcholinesterase, AP = Alkaline phosphatase, AuNPs = Gold Nanoparticles, aGO = Acryloylated Graphene Oxide, BChE = Butyrylcholinesterase, BPA = Bisphenol A, CB = Carbon Black, CB/CP = Carbon Black-Carbon Paste, ChOx = Choline Oxidase, CoPc = Cobalt Phthalocyanine, CS = Chitosan, DDAB = Didodecyldimethyl Ammonium Bromide, DHP = Dihexadecylphosphate, 2,4 D = 2,4-dichlorophenoxyacetic acid, DMF = Dimethyl formamide, EVA = poly(ethylene co-vinyl)acetate, GOx =Glucose Oxidase, GC = Glassy Carbon, ITO = Iridium Tin Oxide, Lac = Laccase, MC = Mesoporous Carbon, OPH = Organophosphorus Hydrolase, OMNiDIP = One MoNomer dual imprinted polymers, PA = Pillar[5]arene, PB = Prussian Blue, PBNPs = Prussian Blue Nanoparticles, Per = Peroxidase, PVDF = Polyvinylidene Fluoride, SPGMA = Star Polymer, SPE = Screen-Printed Electrode, TC = Thiacalix[4]arene, Tyr = Tyrosinase, WS_2 = Tungsten Disulphide, EIS= Electrochemical Impedance Spectroscopy.

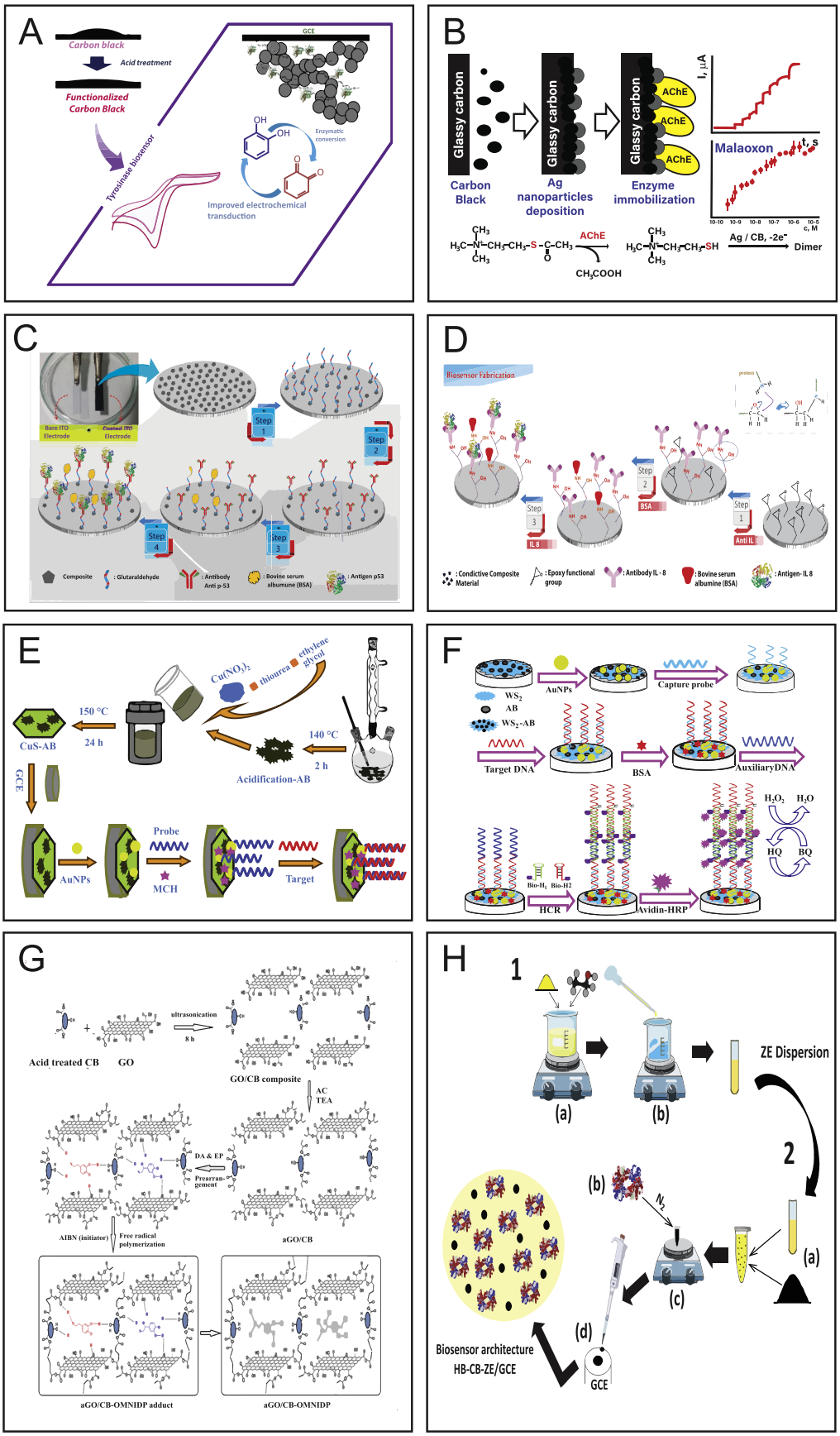

Fig. 3. A) Carbon black and dihexadecylphosphate functionalisation of glassy carbon electrode for tyrosinase biosensor development (Ibanez-Redin et al., 2018). **B)** Modification of a glassy carbon electrode with carbon black and silver nanoparticles for malaoxon detection by evaluating the cholinesterase-enzyme inhibition (Evtugyn et al., 2014). **C)** Immunosensor for p53 detection based on chitosan-super P composite modified ITO electrode (Aydın et al., 2018a). **D)** Immunosensor for IL-8 biomarker detection (Aydın et al., 2018b). **E)** A sequence-specific DNA electrochemical sensor based on acetylene black (Huang et al., 2015). **F)** Acetylene black-based immunosensor fabrication procedure for DNA biosensing (Shuai et al., 2019b). **G)** One MoNomer acryloylated graphene oxide-carbon black composite polymer for dopamine and epinephrine detection (Fatma et al., 2019). **H)** Zein microspheres-carbon black haemoglobin modified glassy carbon electrode for hydrogen peroxide detection (dos Santos et al., 2019).

2014). In the second case, the glassy carbon electrode was modified with the mediator pillar[5]arene and CB, followed by immobilisation of acetylcholinesterase with 1-ethyl-3-(3-dimethylaminopropyl) carbodiimide and N-hydroxysuccinimide. This acetylcholinesterase-based biosensor was able to quantify malaoxon, methyl-paraoxon, carbofuran, and aldicarb with detection limits in standard solutions equal to 4×10^{-12}, 5×10^{-9}, 2×10^{-11} and 6×10^{-10} M, respectively and aldicarb, carbofuran and malathion in spiked peanut and beetroot samples (Shamagsumova et al., 2015).

3.2. Immunosensors

Immunosensors have attracted great interest from scientists, being capable of specific, sensitive, cost-effective, and in-field analysis. Further support comes from nanomaterials, ranging from nanoparticles to graphene, which operate both as electrochemical labels and loading agents for smarter communications between bioreceptors and supports, resulting in improved analytical performances. In literature, some examples of CB-based immunosensors in the label-free configuration have been reported. Suprun et al. (2012) realised a label-free electrochemical immunosensor by immobilising on CB, modified screen-printed electrodes antibodies towards cardiac myoglobin, a key analyte in the diagnosis of myocardial infarction. In details, CB and didodecyldimethyl ammonium bromide were used as a reliable support for direct electron transfer reactions between the screen-printed electrode and Fe(III)-heme proteins (e.g. cytochrome *c*, myoglobin, horseradish peroxidase and cytochromes P450). Well-shaped cyclic voltammograms were generated on this electrode indicating the interesting performance of CB over other nanomaterials, as for example single-walled carbon nanotubes, as well as in comparison with bare electrodes. The peak current variation vs. the logarithm of myoglobin concentration showed linear range from 5 to 500 μM using square wave voltammetry as the detection technique. These data demonstrated that direct electron transfer reactions of heme proteins can also be used for the construction of immunosensors for direct detection of these proteins in biological liquids, becoming a model for myoglobin determination.

More recently, Aydin and co-workers realised label-free electrochemical immunosensors for clinical biomarkers, describing the merits of CB. The first immunosensor encompassed a chitosan/CB layer coated ITO electrode for sensitive and selective detection of tumor marker p53 (Aydın et al., 2018a). This composite demonstrated its ability to improve conductivity as well as to immobilise anti-p53 antibodies through the cross-linking of chitosan and glutaraldehyde. p53 was detected by means of change in impedance during the interaction between anti-p53 antibody and p53 antigen, with a low detection limit of 3 fg/mL and a wide linear range of 0.01–2 pg/mL. This immunosensor also showed stability, repeatability, and applicability in human serum (Fig. 3C).

The second immunosensor has been designed using a similar configuration, based on a disposable ITO electrode surface modified with a composite consisting of CB, polyvinylidene fluoride, and Star polymer material for the electrochemical detection of IL-8 in clinical applications (Aydın et al., 2018b). Thanks to its high conductivity, CB was exploited for the improvement of electron transfer between electrode surface and the analyte. This composite served as an immobilisation support for anti-IL 8 antibodies, which were covalently bound to epoxy groups of star polymers. Under optimum conditions, IL-8 was detected with a low detection limit, 3.3 fg/mL, and a wide linear range, 0.01–3 pg/mL. Saliva and serum samples were analysed to underline the immunosensor suitability in real samples, indicating compatible analytical performances of enzyme-linked immunosorbent assay kit (Fig. 3D).

CB has also been used in the immunosensor for C-reactive protein using hot electron induced electrochemiluminescence as detection technique, which is a method based on the utilisation of hot electrons with energy higher than Fermi energy and the thermal energy of the surrounding phase. The authors configured the immunosensor using an insulating polystyrene layer on the working electrode, which is capable of improving the electron tunnel emission from the graphite flakes and immobilising the biomolecules. However, polystyrene-graphite composite electrodes are characterised by low hot electron induced electrochemiluminescence emission intensity, associated with relatively high background emission, due to the impurities present in the graphite. The authors demonstrated how they overcame of this drawback by using CB, obtaining field emission/tunnel emission currents comparable to the ones observed with carbon nanotubes. A heterogeneous immunoassay at coated polystyrene-CB electrodes was developed using primary antibodies and Tb(III)-chelate labelled secondary antibodies, allowing for a detection limit of 5.3 μg/L (Salminen et al., 2018).

These examples demonstrated the tremendous potential of CB in the development of sensitive and robust immunosensors, even when compared with other nanomaterials such as gold nanoparticles and carbon nanotubes (Table S1), paving the way for further efforts on this topic.

3.3. DNA sensors

Considering the important requirement for advanced analytical tools to monitor biorecognition and interaction events, an impressive number of DNA-based electrochemical sensors have appeared in literature which combine nucleic acids with electrochemical transduction systems, permitting affordable, simple, and effective analysis. As stated by Drummond et al. (2003) "*DNA-based electrochemical sensors exploit a range of different chemistries, but all take advantage of nanoscale interactions between the target in solution, the recognition layer and a solid electrode surface*". Nowadays, the unanswered question is how to further implement these devices to obtain sensitive multiplexed assays for clinical diagnostics of genetic and infectious diseases. Nanotechnology shows potential for responding to this need, by supplying smart nanomaterials able to ameliorate the interactions established between the bioelement and the support. In this context, CB can be considered a good candidate for improving the analytical performances of DNA-based biosensors, in terms of higher sensitivity and reproducibility. As an example, the detection of oxidative DNA damage was achieved by voltammetric analysis by using a glassy carbon electrode covered with CB-adsorbed pillar[5]arene molecules (Kuzin et al., 2018). Thanks to this hybrid coating of pillar[5]arene implemented in the electropolymerized layer of poly(Neutral Red) on the CB particles, the electropolymerization of Neutral Red occurred in the presence of native or oxidatively damaged DNA turned out in the formation of hybrid material, which activity depended on the DNA conditions. The study of DNA and pillar[5]are on redox activity of polymeric dye was carried out by observing an increase in the response in case of DNA damaged by reactive oxygen species. In this configuration CB-pillar[5]arene composite enhanced response and reproducibility.

Acetylene black, a special kind of CB with a porous structure, has been also exploited for the design of DNA-based sensors, thanks to its excellent properties such as excellent electric conductivity, large surface area, high catalytic activity, and strong adsorptive ability. Huang et al. (2015) described the use of acetylene black to modify a glassy carbon electrode in combination with CuS nanosheets and gold nanoparticles for target DNA detection, using a DNA labelled at 5′ end with 6-mercapto-1-hexane and immobilised on the modified electrode through Au–S interaction. After blocking with 6-mercapto-1-hexanol, the formation of a double-stranded structure, due to the binding between the probe DNA and the target DNA on the electrode surface, this allowed for a decrease in the peak current of electrochemical mediator $[Fe(CN)_6]^{3-/4-}$ and the quantification of the target DNA. Under optimal conditions, this DNA sensor showed a detection limit as low as 20 fM ($3\sigma/S$) and a linear range from 0.1 pM to 1 nM, as well as acceptable stability and reproducibility, thanks to the synergistic effect of acetylene black and CuS nanosheets (Fig. 3E).

Shuai et al. (2019b) synthesized a 2-dimensional tungsten disulfide–acetylene black composite to modify, together with gold nanoparticles, a glassy carbon electrode for DNA target recognition. The DNA sensor was designed by immobilising the DNA capture probe by

thiol-gold bonds, followed by hybridisation with the target DNA. The formation of a duplex was estimated by a signal amplification approach to increase the sensitivity by using auxiliary DNA and two DNA hairpins H1 and H2 opened by the recognition probe. Indeed, the double helices, resulting from the hybridization chain reaction, were used to immobilise horseradish peroxidase enzymes for its catalytic *enzymatic* signal-amplification. This DNA sensor provided a good linear response towards DNA concentration ranging from 0.001 pM to 100 pM and a very low detection limit of 0.12 fM, as well as very good selectivity to differentiate the one-base mismatched DNA sequence (Fig. 3F).

The first microRNA-based CB sensor was reported by Yammouri et al. (2017) which fabricated a pencil graphite modified with CB by drop-casting and functionalised with a DNA probe for microRNA-125a detection. To deliver a label free DNA sensor, the electrochemical impedance spectroscopy was selected as the electrochemical technique to quantify the binding between the DNA and microRNA-125a. A low detection limit was found equal to 10 pM (1 pg/mL) with a linear response between 1 nM and 2 μM. The biosensor was also tested in serum samples, indicating its effectiveness in clinical diagnostic assays.

Yammouri et al. (2019) also realised a cost-effective, simple and sensitive electrochemical biosensor for the detection of microRNA-21, which could show an emerging role in cancer diagnosis. Here, the combination of CB with gold nanoparticles was described for the modification of pencil graphite electrode and the consequent immobilisation of a thiolated capture probe (complementary sequence of microRNA-21) labelled with methylene blue. After hybridization with the target microRNA-21, the distance of the labelled capture probe changed with a consequent decrease in the methylene blue response. The biosensor quantified microRNA-21 by differential pulse voltammetry with a limit of detection of 1 fM and a wide linear range between 2.9 fM and 0.7 μM. In addition, good reproducibility, stability and excellent selectivity were achieved, along with satisfactory results when microRNA-21 was analysed in serum. As highlighted in Table S2, CB has shown to be a valuable nanomaterial in the construction of DNA sensors even when compared with DNA sensors based on the use of other nanomaterials including graphene, gold nanoparticles, and gold nanorods.

3.4. Other types of biosensors

Besides the conventional bioreceptors such as enzymes, antibodies and nucleic acids, CB was likewise combined with alternative biological recognition elements or with molecular imprinted polymers, demonstrating, also in these cases, its ability to improve their analytical performances. As an example, imprinted polymers have been exploited in joint conjunction with CB to simultaneously detect dopamine and epinephrine. In this case, a double imprinted polymer platform was realised, which employed a double imprinted monomer acryloylated graphene oxide-CB composite (Fig. 3G). The presence of acid treated CB displayed two major roles, as crosslinker and as electron transfer enhancer. The entire architecture was drop-cast onto a carbon screen-printed electrode. Initially, acidified CB was linked to the graphene oxide sheets. Successively, both the dopamine and epinephrine were added, and the presence of an initiator permitted the entire structure to polymerize, with the target species entrapped. The removal of dopamine and epinephrine was then necessary to complete the double imprinted polymer. The use of differential pulse voltammetry revealed limits of detection equal to 0.028, 0.028, 0.061 and 0.029 ng/mL for dopamine and to 0.017, 0.018, 0.019 and 0.020 ng/mL for epinephrine in water, serum, urine, and pharmaceutical samples, respectively. However, an advantage of the imprinted platform is that the interfering species can be removed by simple water rinsings (Fatma et al., 2019).

Messaoud et al. (2018) reported a screen-printed carbon electrode, modified with an ultrasound assisted magnetic molecularly imprinted polymer, coupled with a gold nanoparticles-carbon black composite. This sensor was applied in order to detect bisphenol A by means of differential pulse voltammetry measurements, obtaining a LOD of 8.8 nM with a linear range up to 10 μM. The sensor, once developed, was successfully applied for the determination of BPA in tap and mineral water samples.

CB was also combined with hemoglobin anchored to zein structured in microspheres, to produce glassy carbon electrodes for the detection of hydrogen peroxide (Fig. 3H). All the modifiers were dispersed in ultrapure water and drop-cast onto the glassy carbon electrode and then dried for 60 min at room temperature. The presence of the zein protein consented the use of a renewable source by creating a friendly environment for immobilising biomolecules, while the presence of CB assured good conductivity and a synergistic effect with the iron atom of hemoglobin. Differential pulse voltammetry allowed the detection of hydrogen peroxide with a linear range from 5 to 100 μM, and a detection limit of 4 μM. This biosensor was applied to quantify hydrogen peroxide in milk, serum, and in commercially-available hydrogen peroxide solutions. The presence of zein from renewable sources and CB, enabled a good immobilisation of hemoglobin, reflected in a high level of stability and selectivity against possible interferents (e.g. sodium nitrate, calcium chloride, tin chloride, glucose) (Dos Santos Pereira et al., 2019).

4. CB-based sensors

Beside biosensor application, CB was largely used in sensor design for both single analyte detection and multianalysis, demonstrating increased sensitivity thanks to its high conductivity, number of defect sites, and surface area.

4.1. Sensors for single analyte detection

Electrochemical detection of specific targets without the use of biocomponent has been carried out for single analyte detection by exploiting the direct electron transfer at CB-based electrodes. Several molecules including hormones, phenolic compounds, and hydrogen peroxide were analysed and different configurations designed with printed, carbon paste or glassy carbon electrodes, using CB by itself or with other nanomaterials such as metallic nanoparticles, carbon nanotubes, graphene, or electrochemical mediators (e.g. Prussian Blue, copper phthalocyanine).

For instance, Talarico and co-workers described the development of screen-printed sensors, modified with CB for phenolic compounds and phosphate quantification, demonstrating the capability of CB to dramatically decrease the applied potential and increase the sensitivity. In addition, in both cases the antifouling properties of CB were demonstrated. In detail, phenolic compounds such as catechol, gallic acid, caffeic acid, and tyrosol were detected with concentration as low as 0.1 μM, 1 μM, 0.8 μM, and 2 μM respectively, with detection limits much lower when compared with the ones obtained in the case of bare electrodes (Talarico et al., 2015a) (Fig. 4A). The electrochemical detection of phenolic compounds using modified CB-electrode (glassy carbon electrode) was also successively demonstrated by Lounasvuori et al. (2018) confirming the enhanced current densities and lower oxidation potentials using glassy carbon electrode modified with CB. In case of phosphate detection, a linear range of 0.5–100 μM was observed with a detection limit of 0.1 μM in batch configuration (Talarico et al., 2015a). This miniaturized sensor was further embedded in an automatable flow system to automatically monitor the electroactive complex obtained from the reaction between phosphate and molybdate (Talarico et al., 2015c). Also in a flow system, the presence of CB led to the quantification of the complex at low potential, being capable of electrocatalytically enhancing the phosphomolybdate complex reduction at +125 mV versus Ag/AgCl, without fouling problems observed in the bare electrode. The flow system allowed for the continuous and long-term amperometric monitoring of phosphate with a low detection limit (6 μM) and good recovery percentages (89–131.5%) in various water sources, highlighting its suitability for in field measurements. Printed electrodes modified with CB have also been applied for mercury

ion detection, exploiting the formation of a non-electroactive complex (thiol–Hg) in the presence of the metal. In this way, the presence of Hg^{2+} provided a decreased thiol response, proportional to the metal amount (Arduini et al., 2011). This CB-based sensor showed a significantly enhanced electrochemical activity with respect to a bare electrode in the case of thiol detection, also improving the sensitivity of metal quantification. A stable response and a linear dependence up to 1×10^{-5} mol L^{-1} for thiocholine and cysteine was observed, and a concentration of mercury as low as 5×10^{-9} mol L^{-1} (1 ppb) was detected.

CB was also used as a modifier to develop modified glassy carbon electrodes (dos Santos et al., 2019; Ławrywianiec et al., 2017). For instance, a CB-modified glassy carbon electrode was fabricated for the detection of the stimulant selegiline by adsorptive stripping voltammetry. The use of CB conferred to the glassy carbon electrode a higher sensitivity, ca. 300-fold higher compared with the un-modified one, and a detection limit ca. 30-fold lower than the bare glassy carbon electrode (dos Santos et al., 2019). Ławrywianiec et al. (2017) developed a glassy carbon electrode modified with a CB layer for bisphenol A measurement, observing a better sensitivity in comparison with a bare electrode and with an electrode modified with graphene and multi-walled nanotubes. The signal arising from bisphenol A oxidation using differential pulse voltammetry, was linear from 0.01 to 3 μM, displaying a detection limit of 3.4 nM (Ławrywianiec et al., 2017).

It is noteworthy that the use of different electrodes, such as printed or glassy carbon, requires a variety of solvents for CB dispersion, including dimethylformamide/water 1:1 (v/v), in the case of printed electrodes, or ethanol, dimethylformamide in the case of glassy carbon electrodes (dos Santos et al., 2019; Deroco et al., 2017). The utilisation of different solvents for CB dispersion does not affect the electrochemical behaviour, which demonstrates the robustness of electrode modification with this nanomaterial. Furthermore, the use of different types of CB (Table 2) demonstrated its huge capability in improving the electroanalytical properties of the (bio)sensors independently of the CB type used, further strengthening their robustness.

CB has also been merged with other nanomaterials including ferroferric oxide (Hou et al., 2014), palladium/nickel (Zhang et al., 2013), silver (Raymundo-Pereira et al., 2016), copper (Carvalho et al., 2013) and ZnO nanoparticles (Rahman et al., 2018) for the detection of several analytes. For instance, Raymundo-Pereira et al. (2017a) modified glassy carbon electrodes with CB decorated with silver nanoparticles, for estriol hormone detection (Fig. 4B). The presence of silver nanoparticles increased both conductivity and electroactive area in comparison with bare glassy carbon electrode and CB-modified one. The synergistic effect of the nanocomposite consented the lowering of ca. 100 mV the overpotential for estriol hormone, which was detected with differential pulse voltammetry linearly from 0.2 to 3 μM with a detection limit of 0.16 μM. The platform was tested in a creek water sample with the same performance as in the official method, i.e. HPLC. The presence of common interferences such as sulphite, nitrite, glucose, amoxicillin, ascorbic acid, levofloxacin, sulfamethazole, acetaminophen, bisphenol A and

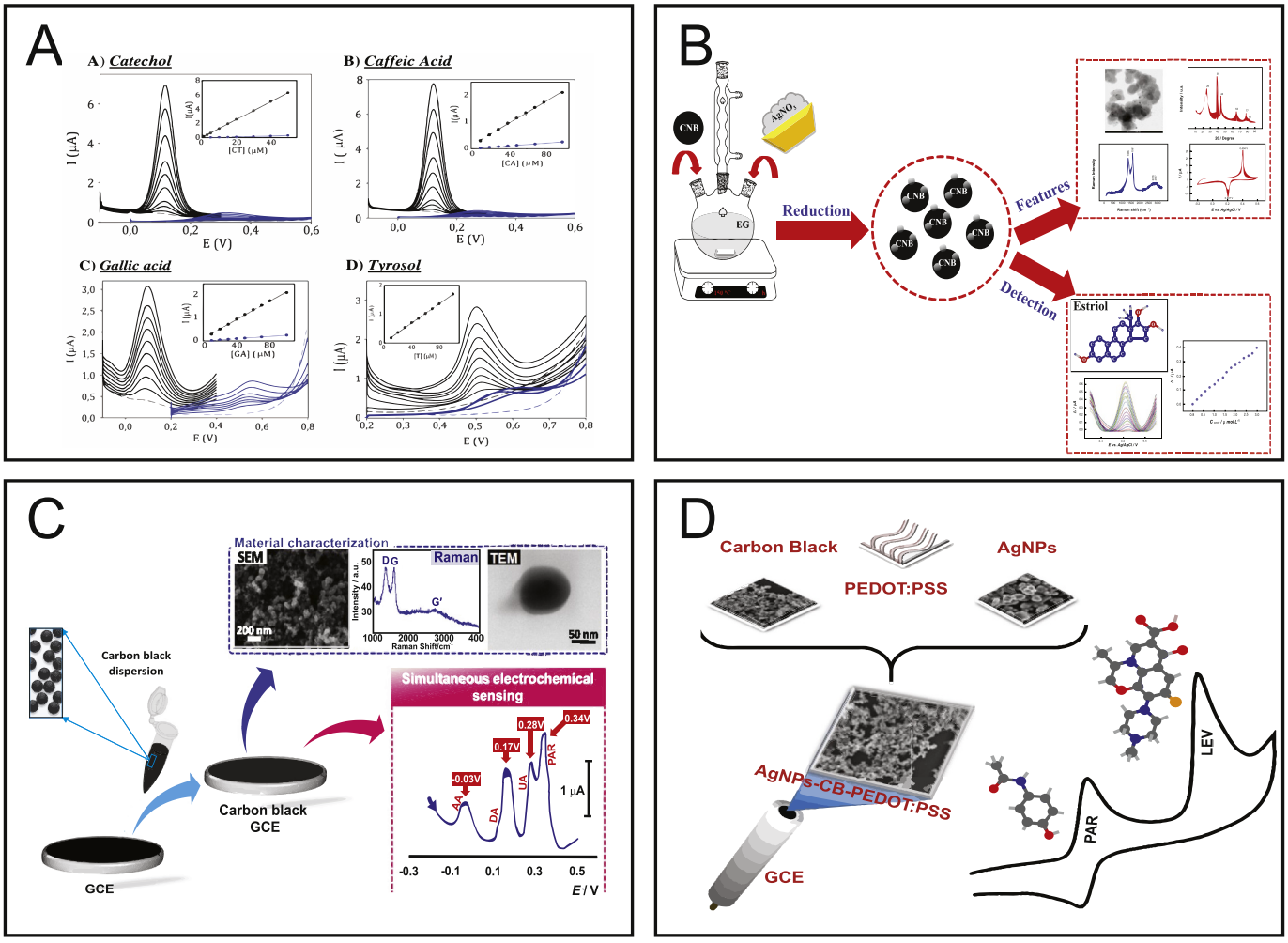

Fig. 4. A) Square wave voltammetry of phenolic compound by using carbon black-modified screen-printed electrode (Talarico et al., 2015a). **B)** Carbon black-sensor platform to detect estriol (Raymundo-Pereira et al., 2017a). **C)** Carbon black film modified glassy carbon electrode for ascorbic acid, dopamine, uric acid and paracetamol detection (Vicentini et al., 2016). **D)** Glassy carbon electrode modified with carbon black, silver nanoparticles, and poly(3, 4-ethylenedioxythiophene)-poly(styrenesulfonate) for paracetamol and levofloxacin detection (Wong et al., 2018a).

17-β-estradiol, did not interfere with the estriol detection.

Screen-printed electrodes modified with CB and gold nanoparticles were developed by Cinti et al. (2014, 2016b) for As(III) and Hg^{2+} detection. The electrodes were modified by depositing one layer of CB and one layer of gold nanoparticles. Good peak intensities were obtained as CB provided a larger loading area for gold nanoparticles. The sensor was tested to detect As(III) trace in drinking water, with satisfactory recovery values (99 ± 9%) (Cinti et al., 2014) and inorganic mercury in both river water and soil (Cinti et al., 2016b).

CB was used to support Au–Pd core-shell nanoparticles within a dihexadecylphosphate film for the development of a hydrazine electrochemical sensor. A glassy carbon electrode was modified by drop-casting a water-based dispersion containing all the above cited modifiers. The customization of the bare electrode enhanced the analytical signal of 87% and the overpotential related to the oxidation of hydrazine resulted in a lowering to ca. 700 mV, essential to avoid the oxidation of occurring interferents. Hydrazine was amperometrically detected in the range of 2.50–88.0 μM with a limit of detection of 1.77 μM (Deroco et al., 2018a).

A CB layer cast on the working electrode surface was exploited in order to electrodeposit the electrocatalyst Prussian Blue on a carbon screen-printed electrode for the enzymeless detection of hydrogen peroxide in Parkinson's disease in vitro model. A dimethylformamide/water 1:1 (v/v) dispersion of CB was drop-cast onto the screen-printed electrode; successively the Prussian blue was grown, and lastly a layer of Nafion was used to improve the stability of the modified platform. A continuous amperometric monitoring system was configured and a −50 mV (vs. Ag) applied. The reduction of hydrogen peroxide produced a current signal that was linear between 200 nM and 1 mM. The platform was applied towards the H_2O_2 sensing in the Neuroblastoma cell line SH-SY5Y, and the presence of Penicilin, Streptavidin, L-Glutamine and Fetal Bovine Serum did not show significant interference (Rojas et al., 2018).

CB was also combined with organic electrochemical mediators by developing customised nanocomposites. As an example, a screen-printed electrode modified with a composite made of copper phthalocyanine, CB and Nafion was applied for the detection of 17β-estradiol. An aqueous dispersion containing all the modifiers was drop-cast onto the carbon working electrode and differential pulse voltammetry was adopted for the determination of the target with a detection limit of 5 nM. This simple and low-cost platform was also tested in river water (S. Paulo State, Brazil) and synthetic urine samples. The sensor showed excellent recovery percentages, ranging from 96 to 107% for both samples, similar to those obtained using the comparative spectrophotometric method, thus demonstrating its reliability as an alternative analytical choice (Wong et al., 2019). Glassy carbon electrodes modified with CB decorated with copper phthalocyanine were designed for trimethoprim antibiotic detection. The authors highlighted that copper phthalocyanine resulted in strong adsorption onto CB via π-π interactions, improving the sensitivity. Under optimized experimental conditions, square wave voltammetry analysis presented two linear relationships in the range of 0.4–1.1 μM and 1.5–6.0 μM with a detection limit of 0.6 μM. The proposed platform was successfully used to detect trimethoprim in natural river water samples (Guaraldo et al., 2019). Smolko et al. (2016) reported a glassy carbon electrode modified with pillar[5]arene dispersed in CB layer for native DNA and organic acids detection by means of cyclic voltammetry measurements. In details, the cyclic voltammetric response of pillar[5]arene was affected by the analyte tested because the presence of native DNA and organic acids decrease and/or increase the cathodic and anodic peak, respectively. This electrochemical sensor was able to detect oxalic, succinic, glycolic, and acetic acid down to 10^{-8} M, and native DNA from fish sperm, chicken erythrocytes, and salmon sperm with a limit of detection equal to 0.2 pg/L, 0.1 pg/L, and 0.5 pg/L respectively.

The important properties of CB as large surface area and high conductivity were also exploited to develop solid-state ion selective electrodes. Glassy carbon electrodes were principally modified by CB to fabricate an ion-to-electron transducer layer with high performance, because CB confers to the potentiometric sensors a long-term potential stability and repeatability. For instance, in 2012 Paczosa-Bator (2012) used for the first time, CB Printex XE2, for the development of a potentiometric sensor for potassium detection, by employing CB as polymeric membrane component or as intermediate layer between the ionophore-containing membrane and glassy carbon electrode. In both cases, a good Nernstian response to potassium detection was observed (59.1–58.8 mV/decade), with detection limits equal to $10^{-6.4}$ M and $10^{-6.1}$ M, respectively. In addition, the same author tested Printex XE2 or Vulcan XC-72 CB as an interlayer between ionophore-membrane and glassy carbon electrode for nitrate measurement, obtaining a detection limit of 2.5×10^{-7} M, which is lower than the one obtained with graphene based electrode (3×10^{-5} M) (Paczosa-Bator, 2014). Paczosa--Bator et al. (2013) applied CB in combination with platinum nanoparticles as intermediate transducer layer for the development of potassium and nitrate solid-state ion-selective electrodes. The potassium- and nitrate-selective electrodes displayed a Nernstian slope, i.e. 57.98 ± 1.02 mV/decade and −58.63 ± 0.24 mV/decade, and a detection limit equal to $10^{-6.1}$ M and $10^{-6.3}$ M, respectively.

The conjunction of CB with other nanomaterials such as carbon nanotubes and MoS_2 has also been reported in literature. For bisphenol A detection, CB was initially combined with carboxylic acid-functionalised multiwalled carbon nanotubes, then dispersed in ethanol and finally drop-cast onto a glassy carbon electrode. The resultant platform displayed satisfactory sensitivity with a linear range varying from 0.1 to 130 μM and with a low detection limit of 0.08 μM. In addition, a long-run stability of 20 days was observed, demonstrating the stability of the CB/multi-walled carbon nanotube modified glassy carbon electrode. The authors applied this device to analyse bottles of drinking water, with recoveries of 90–102%. (Thamilselvan et al., 2019). CB was also used in combination with MoS_2 to produce a high-performance nanohybrid sensor for cocoa catechin determination, approaching an extraction-free strategy. Two separated dispersions of CB and MoS_2 were prepared in dimethylformamide/water 1:1 (v/v), and successively drop-cast onto a carbon screen-printed electrode. Differential pulse voltammetry was used as the electrochemical method and the presence of the nanohybrid composite produced a sensitivity enhancement of 100-fold compared with the unmodified screen-printed electrode. The voltammetric response appeared linear from 0.12 to 25 μM. Epicatechin, catechin and epigallocatechin were detected using the extraction-free approach in cocoa powder samples, made possible thanks to the antifouling properties of the modifier (della Pelle et al., 2019).

The reported literature highlights the advantage of using CB as stand alone nanomodifier or combined with other materials such as MoS_2, carbon nanotubes, Prussian Blue, gold and silver nanoparticles, potato starch (Delgado et al., 2018), nanoporous copper and Nafion (Mei et al., 2016), demonstrating the capability that CB has in improving other nanomaterial properties.

4.2. Sensors for multianalysis detection

The fascinating electrochemical properties of CB have also been exploited in the design of sensors for the multianalysis of a variety of electroactive analytes such as pharmaceutical compounds, emerging pollutants, ascorbic acid, dopamine, and uric acid, mainly by using electrodes modified with CB alone or in combination with graphene, MoS_2, β-cyclodextrin, and metallic nanoparticles.

For example, the use of CB suspended in dimethylformamide and successively drop-cast onto a glassy carbon electrode permitted the simultaneous detection of two emerging pollutants, namely hydroquinone and paracetamol. The measurements were carried out by experiments in differential pulse voltammetry at a low overpotential of 67 and 341 mV, respectively for hydroquinone and paracetamol. The linearity range for the two species was found to be made up of a range between 80 nM and 230 μM. In addition, the detection limits were calculated as being equal to 13 and 8 nM, for hydroquinone and paracetamol

(Raymundo-Pereira et al., 2017b).

Amoxicillin and nimesulide were detected using CB included in a dihexadecylphosphate film. The glassy carbon electrode was drop-cast with a water-based dispersion containing both the CB to strengthen the electrochemical signal and dihexadecylphosphate, which had the role of stabilizing the surface of the electrode. The use of square-wave voltammetry demonstrated a separation of ca. 180 mV between the oxidation peak potentials of the two analytes, and the detection limits obtained for amoxicillin and nimesulide were calculated as being equal to 0.12 and 0.016 μM, respectively (Deroco et al., 2018b).

CB dispersed in dimethylformamide was drop-cast onto a glassy carbon electrode and served as the basis for the layering of a carboxymethyl-botryosphaeran film to simultaneously detect phenolic compounds. The combination of the carbohydrate biopolymer and CB enabled detection by differential pulse voltammetry of dopamine and paracetamol simultaneously in the concentration range of 0.099–2.9 and 0.70–19 μM, with limits of detection of 0.013 and 0.11 μM respectively. These phenolic compounds were detected in biological fluids, by taking advantage of the anodic and cathodic currents, for the measurements in urine and cerebrospinal fluid respectively, both without any significant matrix effect (Eisele et al., 2019).

For the simultaneous electrochemical determination of ascorbic acid, dopamine, uric acid, and paracetamol, a modified glassy carbon electrode CB film was evaluated (Vicentini et al., 2016). The structural characterisation of the composite by transmission electron microscopy, scanning electron microscopy, and Raman spectroscopy showed good distribution of the CB with a nanoscale particle size, while the electrochemical analysis by cyclic voltammetry demonstrated its high electrocatalytic performance. Detection limits of 3.03×10^{-8}, 5.24×10^{-8}, 4.07×10^{-8} and 4.53×10^{-8} mol L^{-1} were obtained for ascorbic acid, dopamine, uric acid, and paracetamol, respectively. The application of this sensor was also achieved in biological samples with excellent recovery values for all the analytes (Fig. 4C).

Paracetamol and codeine were simultaneously analysed in pharmaceuticals and human body fluids. A glassy carbon electrode modified with CB and nickel oxide nanoparticles within a dihexadecylphosphate film was used. (Deroco et al., 2015). Linear concentration ranges from 3.0 to 47.8 μmol L^{-1} for paracetamol and from 0.83 to 38.3 μmol L^{-1} for codeine were obtained in standard solution, as well as their determination in two different commercial pharmaceutical samples. This was achieved by interpolation in the respective previously obtained analytical curves, with no significant differences from the reference HPLC method.

A similar sensor based on a glassy carbon electrode modified with reduced graphene oxide and CB in a chitosan film was exploited for the simultaneous determination of dopamine and paracetamol (Baccarin et al., 2017). Here, the combination of the two nanomaterials with chitosan provided a stable dispersion that was successfully used as an electroactive layer. Indeed, good electroanalytical features arose with detection limits of 2.0×10^{-7} and 5.3×10^{-8} mol L^{-1} and linear range from 3.2×10^{-6} to 3.2×10^{-5} mol L^{-1} and from 2.8×10^{-6} to 1.9×10^{-5} mol L^{-1} for dopamine and paracetamol, respectively. Furthermore, the main advantages were highlighted as including simple preparation, low cost of the nanomaterials used, and a fast response.

Silver nanoparticles and poly(3,4-ethylenedioxythiophene)-poly (styrenesulfonate) were likewise combined to CB to modify a glassy carbon electrode in the design of a voltammetric sensor for the simultaneous determination of paracetamol and levofloxacin (Wong et al., 2018a). The electrochemical behaviours of these analytes were evaluated by cyclic voltammetry in a potential range from 0 to 1.2 V, obtaining higher oxidation peaks by a factor of 5.7 for paracetamol, and 12 for levofloxacin with respect to a bare electrode, with detection limits of 1.2×10^{-8} and 1.4×10^{-8} mol L^{-1} and linear ranges of 6.2×10^{-7}-7.1×10^{-6} mol L^{-1} and 6.7×10^{-7}-1.2×10^{-5} mol L^{-1}, respectively. In addition, the sensor showed good stability, reproducibility, and repeatability, any interference in the presence of other compounds, and suitable application in both clinical (i.e. synthetic urine) and environmental (i.e. river water) samples, with recoveries close to 100% (Fig. 4D).

CB, in conjunction with graphene oxide, copper nanoparticles, and poly(3,4-ethylenedioxythiophene)-poly(styrenesulfonate) as electrode materials, was likewise realised for the simultaneous analysis of isoproterenol, acetaminophen, folic acid, propranolol, and caffeine. This sensor was electrochemically characterised using the potassium ferricyanide as redox probe, fast electron transfer kinetics and a higher electroactive surface area were observed. Well defined and resolved anodic peaks were achieved by square-wave voltammetry for all the selected target analytes, with peak-to-peak potential separation no less than 170 mV. A mixture of these analytes went on to be analysed with linear range and limit of detection at μmolar ranges (Wong et al., 2018b).

An alternative noncovalent and eco-friendly approach was proposed for the preparation of a carbon-black/β-cyclodextrin nanocomposite to modify screen-printed carbon electrodes for the simultaneous determination of the anticancer drug flutamide and the environmental pollutant 4-nitrophenol (Kubendhiran et al., 2018). The electrochemical performance of this sensor was augmented thanks to CB's high conductivity, as well as to the different binding strengths of these analytes to the host β-cyclodextrin, and finally, to the different reduction potentials of the nitroaromatic compounds. Indeed, this sensor configuration exhibited high sensitivity, selectivity, and reproducibility, with linear ranges 0.05–158.3 μM and 0.125–225.8 μM and low detection limits of 0.016 μM and 0.040 μM for flutamide and 4-nitrophenol, respectively.

Ortho-diphenols oleuropein and hydroxytyrosol were detected in a carbon screen-printed electrode modified with a composite, made up of CB and MoS_2. The electrode was modified by drop-casting a few microliters of a dispersion of CB-MoS_2 which improved charge-transfer features of the platform, lowered charge-transfer resistance and enhanced the electrocatalysis: the peak-to-peak separation in the presence of ferricyanide as the redox probe, decreased from 280 to 185 and 130 mV, for bare, CB-, and CB-MoS_2 modified electrode, respectively. The two diphenols were detected via difference pulse voltammetry which obtained the following results: oleuropein was detected in the 0.3–30 μM range with a detection limit of 0.1 μM, while hydroxytyrosol provided a linear output in the 2–100 μM range with a 1 μM detection limit. The effectiveness of the developed platform was compared with the reference HPLC-UV method, exhibiting a high correlation ($r = 0.995$, $p < 0.05$) (Rojas et al., 2019).

5. Paper-based CB-modified (bio)sensors

While CB can be considered as a more sustainable nanomaterial than the most widely known graphene and carbon nanotubes, being cheaper and not requiring any chemical treatment, another traditional and sustainable material has been re-discovered in the field of electrochemical biosensors: paper. The combination of paper with CB, as a smart support for the printing of eco-friendly electrodes, is emerging to design sustainable devices.

Paper's valuable features include foldability, porosity, and easy functionalisation confer unprecedented potential in the realisation of electrochemical paper-based analytical devices (ePADs), being capable of:

i) using a minimum amount of reagents, as a few μL film present in the cellulose network is the working solution;
ii) treating the sample with no further steps and reagents (Cinti et al., 2018b) ;
iii) providing cheap measurement using a sensor with a cost lower than 1 € (Cinti et al., 2017b);
iv) being incinerated after the measurement thus reducing waste.

However, a lower sensitivity compared to a classical configuration can be observed, the analyte diffusion is hindered by the cellulose network, though nanomaterials have been used to overcome this drawback. The first applications of CB in ePAD have been reported in case of sensor for phosphate detection (Fig. 5A). The detection was carried out

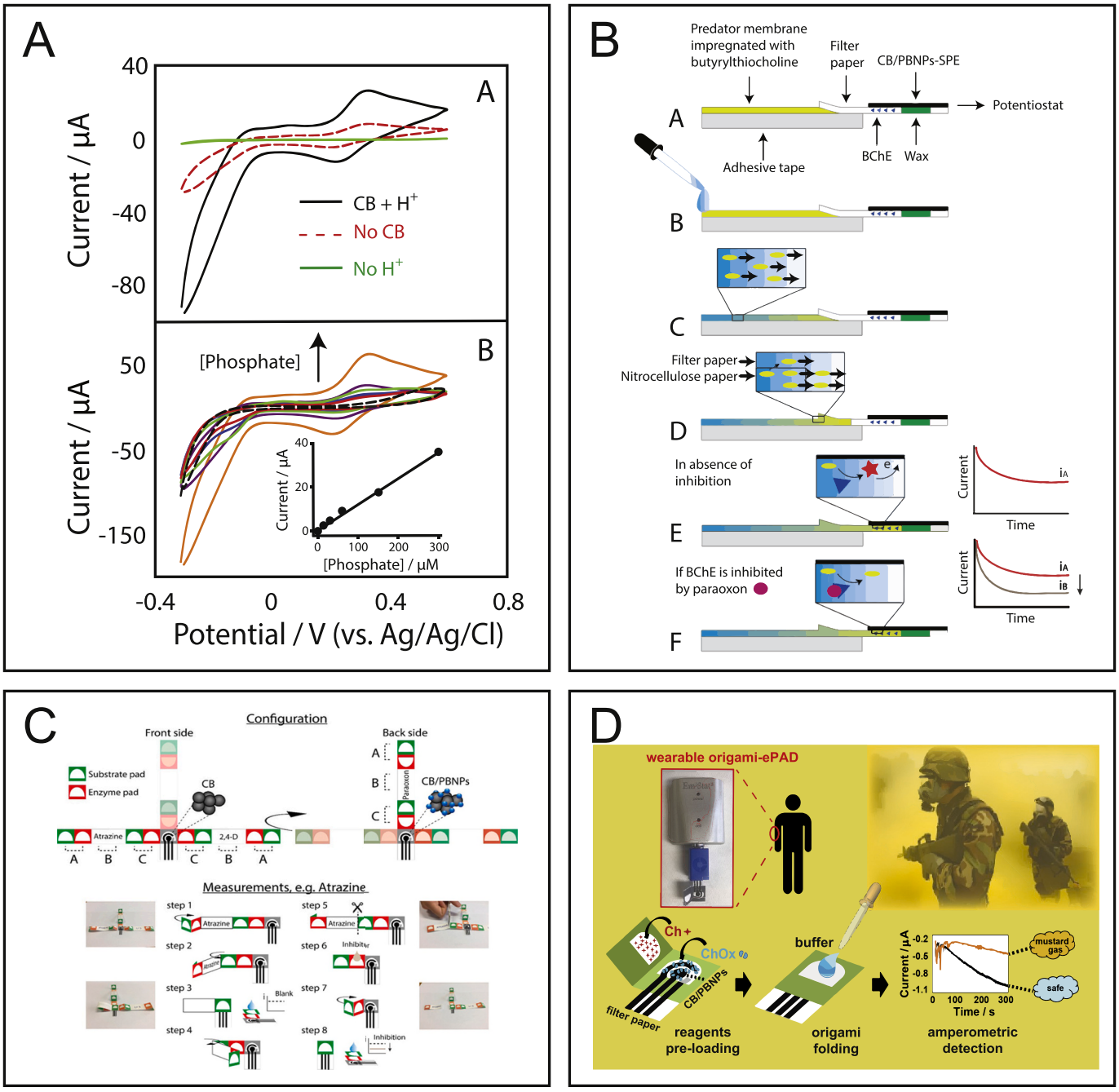

Fig. 5. A) Carbon black-modified paper-based sensor for phosphate detection (Cinti et al., 2016c). **B)** Carbon black-Prussian Blue nanoparticles modified paper-based biosensor for organophosphate detection in surface water (Cinti et al., 2017c). **C)** Combined origami paper-based biosensors for analysis of multiclass pesticides (Arduini et al., 2019). **D)** Wearable origami paper-based biosensor for sulphur mustard detection in gas phase (Colozza et al., 2019). (For interpretation of the references to colour in this figure legend, the reader is referred to the Web version of this article.)

following the reaction of phosphate with molybdate ions in acidic media (Talarico et al., 2015b, 2015c). The electrochemical measurement of generated electroactive phosphomolybdic complex at low applied potential was characterised by low sensitivity and fouling problem, using a bare graphite-based electrode. The use of CB permitted highly sensitive quantification of phosphate at an applied potential of +300 mV without working electrode surface fouling, with a detection limit of 4 µM and a linear range up to 300 µM. Partnering paper with CB led to a reagentless phosphate sensor, because all reagents were loaded onto a paper network; in addition, high sensitivity and reproducibility were obtained thanks to the use of CB in modifying the ink during the printing process (Cinti et al., 2016c). After the first use of CB in paper-based sensor, various enzymatic paper-based biosensors have been developed. Cinti et al. (2017c) developed a butyrylcholinesterase biosensor using two paper strips for the detection of the enzymatic activity in the absence, and in the presence, of the inhibitor to detect nerve agents in surface water samples. The enzymatic by-product thiocholine was accurately detected in the paper-based sensor thanks to the presence of CB and Prussian blue nanocomposite, added in the ink, which was used to print the working electrode surface. Its ability to electrocatalyse the oxidation of thiocholine at low applied potential meant that also in this case, the fouling drawback was avoided. To deliver a reagent free biosensor, the enzyme was loaded onto the filter paper in close proximity to the working electrode surface, while the substrate was loaded onto the nitrocellulose strip. Adding the untreated and undiluted water sample and/or distilled water allowed the enzymatic substrate to flow; paraoxon as

organophosphate model was detected down ppb levels (Fig. 5B).

A multi-class pesticide analysis was reported using an origami biosensor, made up of several filter paper-based pads and electrodes printed on office paper (Arduini et al., 2019). Folding, unfolding, wetting with distilled water, and cutting the pads allowed for the detection of atrazine deriving from triazine herbicide, 2,4-dichlorophenoxyacetic acid from phenoxy herbicides, and paraxon from organophosphorus insecticides, in undiluted and untreated river water samples. The detection was based on the residual enzymatic activity quantification as these compounds are able to inhibit tyrosinase, alkaline phosphatase, and butyrylcholinesterase, respectively. Using different configurations of the pads, and two types of office paper screen-printed electrodes, which had been modified with CB and/or Prussian Blue nanoparticles, the foldable device was capable of assessing the different classes of pesticides in river water samples (Fig. 5C). The office-paper modified with CB and Prussian Blue nanoparticles was also combined with two filter-paper pads containing choline oxidase as bioreceptor and choline as enzymatic substrate to detect mustard agent in the solution and gas phase (Fig. 5D). The choice of this enzyme is due to the capability of these chemical warfare agents to inhibit choline oxidase in a reversible way (Colozza et al., 2018). In this case, CB-based nanocomposite was used to electrocatalyse the reduction of hydrogen peroxide, the enzymatic by-product of the choline oxidase enzyme. The vertical origami configuration combining CB-based printed electrode and filter pads demonstrated its effectiveness in rapid and real-time detection of real sulphur mustard, obtaining limits of detection equal to 1 mM and 0.019 g $\times$ min/m^3 for liquid and aerosol phase, respectively (Colozza et al., 2019).

6. Conclusions and future perspectives

The use of nanomaterials in (bio)sensor design has greatly improved their analytical performance, the main challenges related to sensor commercialisation have been overcome, thus allowing for their practical application in several sectors. Among nanomaterials, metallic nanoparticles have covered a central role in the development of electrochemical biosensors by exploiting the nanodimensions to improve the electron transfer as well as loading the biocomponents (Zeng et al., 2019; Cai et al., 2018; Lv et al., 2018; Qiu et al., 2018). In the field of carbon nanomaterials, the use of carbon nanotubes in electrochemical biosensors has recently fallen out of favour, thanks to graphene's capability of improving the electrochemical responses, to cleverly immobilise the biocomponent, and to work as a smart label. CB is gaining great interest due to its electrocatalytic properties and biocompatibility, becoming a fashionable candidate for sustainable and smart (bio)sensor development. Nowadays most CB-based sensing systems are principally sensors, but in the recent years, a sharp increase of publications have been observed in the development of enzymatic, immuno and DNA biosensors (Fig. 1 and Table 2).

In all these configurations, CB has demonstrated unique electroanalytical properties in terms of increased signal/noise ratio, decreased applied potential for redox reactions, and antifouling ability, as well as its compatibility in working in cooperation with bio-components. The use of different CB types and batches leads to an improved electrochemical response in any case, which demonstrates the robustness of this nanomaterial. However, at the state of the art, one of the main disadvantages is that these outstanding features are not deeply understood; they can probably be ascribed to nanodimensions, the onion-like structure, and the high number of defect sites. For CB-based biosensor fabrication, no complicated chemistry is required thanks to the possibility of easily preparing stable dispersions, even if in the case of aqueous solution the addition of polymers (e.g. chitosan) is required. In addition, CB can be "used as it is, from a commercial supplier" as asserted by the Pumera group (Wong et al., 2012). Cost-effectiveness (c. a. 1 €/Kg) represents a further merit for an affordable electrochemical device development. These aspects make CB a next generation material with eco-friendly features in terms of costs and environmental impact.

In the era of sustainability, every scientist has to follow a sustainable vision. With this aim, paper has recently been readopted to design electrochemical paper-based analytical devices, becoming a green tool with reduced reagent consumption and easier sample treatment. Likewise, we are confident that CB can re-emerge as a cost effective and attractive nanomaterial for the development of electrochemical (bio) sensors, by expanding its applications merely relegated, in recent years, to gas sensors and fuel cells. In this review we have described studies that demonstrate the suitability of CB in biosensor design, therefore, why not use this nanomaterial in the development of future electrochemical (bio)sensors?

Declaration of competing interest

The authors declare that they have no known competing financial interests or personal relationships that could have appeared to influence the work reported in this paper.

Acknowledgements

This work was supported by ERANETMED project NanoSWS and Bilateral Agreement Italy- Morocco AlgaeCB.

Appendix A. Supplementary data

Supplementary data to this article can be found online at https://doi.org/10.1016/j.bios.2020.112033.

References

Al-Hartomy, O.A., Ibrahim, M.A., Al-Ghamdi, A.A., Dishovsky, N., Slavcheva, D., Iliev, V., El-Tantawy, F., 2011. Kaut. Gummi. Kunstst 64, 33–39.
Al-Hartomy, O.A., Al-Ghamdi, A., Al-Solamy, F., Dishovsky, N., Mihaylov, M., Ivanov, M., El-Tantawy, F., 2012. Res. Rev. Polym. 3, 93–101.
Alcantara, R., Jimenez-Mateos, L.M., Lavela, P., Tirado, J.L., 2001. Electrochem. Comm. 3, 639–642.
Alwarappan, S., Erdem, A., Liu, C., Li, C.Z., 2009. J. Phys. Chem. C 113, 8853–8857.
Alwarappan, S., Liu, C., Kumar, A., Li, C.Z., 2010. J. Phys. Chem. C 114, 12920–12924.
Alwarappan, S., Boyapalle, S., Kumar, A., Li, C.Z., Mohapatra, S., 2012a. J. Phys. Chem. C 116, 6556–6559.
Alwarappan, S., Cissell, K., Dixit, S., Li, C.Z., Mohapatra, S., 2012b. J. Electroanal. Chem. 686, 69–72.
Amine, A., Arduini, F., Moscone, D., Palleschi, G., 2016. Biosens. Bioelectron. 76, 180–194.
Arduini, F., Amine, A., 2013. Biosensors based on enzyme inhibition. In: Biosensors Based on Aptamers and Enzymes. Springer, Berlin, Heidelberg, pp. 299–326.
Arduini, F., Giorgio, F.D., Amine, A., Cataldo, F., Moscone, D., Palleschi, G., 2010a. Anal. Lett. 43, 1688–1702.
Arduini, F., Amine, A., Majorani, C., Di Giorgio, F., De Felicis, D., Cataldo, F., Moscone, D., Palleschi, G., 2010b. Electrochem. Commun. 12, 346–350.
Arduini, F., Majorani, C., Amine, A., Moscone, D., Palleschi, G., 2011. Electrochim. Acta 56, 4209–4215.
Arduini, F., Di Nardo, F., Amine, A., Micheli, L., Palleschi, G., Moscone, D., 2012. Electroanal 24, 743–751.
Arduini, F., Zanardi, C., Cinti, S., Terzi, F., Moscone, D., Palleschi, G., Seeber, R., 2015a. Sens. Actuat. B212, 536–543.
Arduini, F., Forchielli, M., Amine, A., Neagu, D., Cacciotti, I., Nanni, F., Moscone, D., Palleschi, G., 2015b. Microchim. Acta 182, 643–651.
Arduini, F., Forchielli, M., Scognamiglio, V., Nikolaevna, K., Moscone, D., 2017. Sensors 17, 34.
Arduini, F., Cinti, S., Caratelli, V., Amendola, L., Palleschi, G., Moscone, D., 2019. Biosens. Bioelectron. 126, 346–354.
Aydın, E.B., Aydın, M., Sezgintürk, M.K., 2018a. Biosens. Bioelectron. 121, 80–89.
Aydın, M., Aydın, E.B., Sezgintürk, M.K., 2018b. Biosens. Bioelectron. 117, 720–728.
Baccarin, M., Santos, F.A., Vicentini, F.C., Zucolotto, V., Janegitz, B.C., Fatibello-Filho, O., 2017. J. Electroanal. Chem. 799, 436–443.
Cai, G., Yu, Z., Ren, R., Tang, D., 2018. ACS Sens. 3, 632–639.
Calegari, F., de Souza, L.P., Barsan, M.M., Brett, C.M., Marcolino-Junior, L.H., Bergamini, M.F., 2017. Sensor. Actuat. B. 253, 10–18.
Carvalho, R.C., Mandil, A., Prathish, K.P., Amine, A., Brett, C.M., 2013. Electroanal 25, 903–913.
Cinti, S., Politi, S., Moscone, D., Palleschi, G., Arduini, F., 2014. Electroanal 26, 931–939.
Cinti, S., Arduini, F., Carbone, M., Sansone, L., Cacciotti, I., Moscone, D., Palleschi, G., 2015. Electroanal 27, 2230–2238.
Cinti, S., Neagu, D., Carbone, M., Cacciotti, I., Moscone, D., Arduini, F., 2016a. Electrochim. Acta 188, 574–581.

Cinti, S., Santella, F., Moscone, D., Arduini, F., 2016b. Environ. Sci. Pollut. Res. 23, 8192–8199.
Cinti, S., Talarico, D., Palleschi, G., Moscone, D., Arduini, F., 2016c. Anal. Chim. Acta 919, 78–84.
Cinti, S., Mazzaracchio, V., Cacciotti, I., Moscone, D., Arduini, F., 2017a. Sensors 17, 2267.
Cinti, S., De Lellis, B., Moscone, D., Arduini, F., 2017b. Sensor. Actuat. B-Chem. 253, 1199–1206.
Cinti, S., Minotti, C., Moscone, D., Palleschi, G., Arduini, F., 2017c. Biosens. Bioelectron. 93, 46–51.
Cinti, S., Fiore, L., Massoud, R., Cortese, C., Moscone, D., Palleschi, G., Arduini, F., 2018a. Talanta 179, 186–192.
Cinti, S., Colozza, N., Cacciotti, I., Moscone, D., Polomoshnov, M., Sowade, E., Baumann, R.R., Arduini, F., 2018b. Sensor. Actuat. B. 265, 155–160.
Cinti, S., Moscone, D., Arduini, F., 2019. Nat. Protoc. 14, 2437–2451.
Colozza, N., Kehe, K., Popp, T., Steinritz, D., Moscone, D., Arduini, F., 2018. Environ. Sci. Pollut. R 1–12.
Colozza, N., Kehe, K., Dionisi, G., Popp, T., Tsoutsoulopoulos, A., Steinritz, D., Moscone, M., Arduini, F., 2019. Biosens. Bioelectron. 129, 15–23.
Delgado, K.P., Raymundo-Pereira, P.A., Campos, A.M., Oliveira Jr., O.N., Janegitz, B.C., 2018. Electroanal 30, 2153–2159.
Della Pelle, F., Del Carlo, M., Sergi, M., Compagnone, D., Escarpa, A., 2016. Microchim. Acta 183, 3143–3149.
Della Pelle, F., Di Battista, R., Vazquez, L., Palomares, F.J., Del Carlo, M., Sergi, M., Compagnone, D., Escarpa, A., 2017. Appl. Mater. Today 9, 29–36.
Della Pelle, F., Rojas, D., Scroccarello, A., Del Carlo, M., Ferraro, G., Di Mattia, C., Martuscelli, M., Escarpa, A., Compagnone, D., 2019. Sensor. Actuat. B. 296, 126651.
Deroco, P.B., Vicentini, F.C., Fatibello-Filho, O., 2015. Electroanal 27, 2214–2220.
Deroco, P.B., Lourencao, B.C., Fatibello-Filho, O., 2017. Microchem. J. 133, 188–194.
Deroco, P.B., Melo, I.G., Silva, L.S., Eguiluz, K.I., Salazar-Banda, G.R., Fatibello-Filho, O., 2018a. Sensor. Actuat. B. 256, 535–542.
Deroco, P.B., Rocha-Filho, R.C., Fatibello-Filho, O., 2018b. Talanta 179, 115–123.
Dominko, R., Gaberscek, M., Drofenih, J., Bele, M., Jamnik, J., 2003. Electrochim. Acta 48, 3709–3717.
Donnet, J.B., Custodéro, E., Wang, T.K., Hennebert, G., 2002. Carbon 40, 163–167.
dos Santos, W.T., Amin, H.M., Compton, R.G., 2019. Sensor. Actuat. B. 279, 433–439.
dos Santos Pereira, T., de Oliveira, G.C.M., Santos, F.A., Raymundo-Pereira, P.A., Oliveira Jr., O.N., Janegitz, B.C., 2019. Talanta 194, 737–744.
Drummond, T.G., Hill, M.G., Barton, J.K., 2003. Nat. Biotechnol. 21, 1192.
Eisele, A.P.P., Valezi, C.F., Mazziero, T., Dekker, R.F., Barbosa-Dekker, A.M., Sartori, E. R., 2019. Sensor. Actuat. B. 287, 18–26.
Escarpa, A., 2012. Chem. Rec. 12, 72–91.
Evtugyn, G.A., Shamagsumova, R.V., Padnya, P.V., Stoikov, I.I., Antipin, I.S., 2014. Talanta 127, 9–17.
Fatma, S., Prasad, B.B., Jaiswal, S., Singh, R., Singh, K., 2019. Biosens. Bioelectron. 135, 36–44.
Geim, A.K., Novoselov, K.S., 2010. The rise of graphene. In: Nanoscience and Technology: A Collection of Reviews from Nature Journals, pp. 11–19.
Guaraldo, T.T., Goulart, L.A., Moraes, F.C., Lanza, M.R., 2019. Appl. Surf. Sci. 470, 555–564.
Hocevar, S.B., Ogorevc, B., 2007. Talanta 74, 405–411.
Hopkin, A.R., Lewis, N.S., 2001. Anal. Chem. 73, 884–892.
Hou, C., Tang, W., Zhang, C., Wang, Y., Zhu, N., 2014. Electrochim. Acta 144, 324–331. https://www.mt.com/ch/it/home/supportive_content/matchar_apps/MatChar_HB457.html.
Huang, K.J., Liu, Y.J., Zhang, J.Z., Liu, Y.M., 2015. Sensor. Actuat. B. 209, 570–578.
Ibáñez-Redín, G., Silva, T.A., Vicentini, F.C., Fatibello-Filho, O., 2018. Enzyme Microb. Tech. 116, 41–47.
Iijima, S., 1991. Nature 354, 56.
Kesavan, S., Gowthaman, N.S.K., Alwarappan, S., John, S.A., 2019. Sens. Actuat. B. 278, 46–54.
Kubendhiran, S., Sakthivel, R., Chen, S.M., Mutharani, B., Chen, T.W., 2018. Anal. Chem. 90, 6283–6291.
Kuzin, Y., Kappo, D., Porfireva, A., Shurpik, D., Stoikov, I., Evtugyn, G., Hianik, T., 2018. Sensors 18, 3489.
Lee, J.H., Park, J.Y., Min, K., Cha, H.J., Choi, S.S., Yoo, Y.J., 2010. Biosens. Bioelectron. 25, 1566–1570.
Li, Q., Zhang, X., Wu, G., Xu, S., Wu, C., 2007. Ultrason. Sonochem. 14, 225.
Liberti, A., Morgia, C., Mascini, M., 1985. Anal. Chem. Acta 173, 157–164.
Lo, T.W., Aldous, L., Compton, R.G., 2012. Sensor. Actuat. B. 162, 361–368.
Lounasvuori, M.M., Kelly, D., Foord, J.S., 2018. Carbon 129, 252–257.
Lowinsohn, D., Gan, P., Tschulik, K., Foord, J.S., Compton, R.G., 2013. Electroanal 25, 2435–2444.
Lv, S., Zhang, K., Zeng, Y., Tang, D., 2018. Anal. Chem. 90, 7086–7093.
Malha, S.I.R., Mandli, J., Ourari, A., Amine, A., 2013. Electroanal 25, 2289–2297.
Malha, S.I.R., Lahcen, A.A., Arduini, F., Ourari, A., Amine, A., 2016. Electroanal 28, 1044–1051.
Martinez-Alvarez, O., Miranda-Hernandez, M., 2008. Carbon-Sci. Tech. 1, 30–38.
Mattos, G.J., Moraes, J.T., Barbosa, E.C., Camargo, P.H., Dekker, R.F., Barbosa-Dekker, A.M., Sartori, E.R., 2019. Bioelectrochemistry 129, 116–123.
Mazzaracchio, V., Tomei, M.R., Cacciotti, I., Chiodoni, A., Novara, C., Castellino, M., Scordo, G., Amine, A., Moscone, D., Arduini, F., 2019. Electrochim. Acta 317, 673–683.
Mei, L., Zhang, P., Chen, J., Chen, D., Quan, Y., Gu, N., Zhang, G., Cui, R., 2016. Microchim. Acta 183, 1359–1365.
Messaoud, N.B., Lahcen, A.A., Dridi, C., Amine, A., 2018. Sensor. Actuat. B. 276, 304–312.
Mita, D.G., Attanasio, A., Arduini, F., Diano, N., Grano, V., Bencivenga, U., Rossi, F., Amine, A., Moscone, D., 2007. Biosens. Bioelectron. 23, 60–65.
Nadifiyine, S., Haddam, M., Mandli, J., Chadel, S., Blanchard, C.C., Marty, J.L., Amine, A., 2013. Anal. Lett. 46, 2705–2726.
Pacheco, M.R., Barbosa, S.C., Quadrado, R.F.N., Fajardo, A.R., Dias, D., 2019. Anal. Bioanal. Chem. 411, 3269–3280.
Paczosa-Bator, B., 2012. Talanta 93, 424–427.
Paczosa-Bator, B., 2014. Microchim. Acta 181, 1093–1099.
Paczosa-Bator, B., Cabaj, L., Piech, R., Skupień, K., 2013. Anal. Chem. 85, 10255–10261.
Portaccio, M., Di Tuoro, D., Arduini, F., Moscone, D., Cammarota, M., Mita, D.G., Lepore, M., 2013. Electrochim. Acta 109, 340–347.
Qiu, Z., Shu, J., Liu, J., Tang, D., 2018. Anal. Chem. 91, 1260–1268.
Rahman, M.M., Alam, M.M., Asiri, A.M., 2018. J. Ind. Eng. Chem. 65, 300–308.
Raymundo-Pereira, P.A., Campos, A.M., Prado, T.M., Furini, L.N., Boas, N.V., Calegaro, M.L., Machado, S.A., 2016. Anal. Chim. Acta 926, 88–98.
Raymundo-Pereira, P.A., Campos, A.M., Vicentini, F.C., Janegitz, B.C., Mendonça, C.D., Furini, L.N., Boas, N.V., Calegaro, M.L., Costantino, C.J., Machado, S.A., Oliveira Jr., O.N., 2017a. Talanta 174, 652–659.
Raymundo-Pereira, P.A., Campos, A.M., Mendonça, C.D., Calegaro, M.L., Machado, S.A., Oliveira Jr., O.N., 2017b. Sensor. Actuat. B 252, 165–174.
Razumiene, J., Barkauskas, J., Kubilius, V., Meskys, R., Laurinavicius, V., 2005. Talanta 67, 783–790.
Richter, E.M., Rocha, D.P., Cardoso, R.M., Keefe, E.M., Foster, C.W., Munoz, R.A., Banks, C.E., 2019. Anal. Chem. 91, 12844–12851.
Rojas, D., Della Pelle, F., Del Carlo, M., d'Angelo, M., Dominguez-Benot, R., Cimini, A., Escarpa, A., Compagnone, D., 2018. Sensor. Actuat. B. 275, 402–408.
Rojas, D., Della Pelle, F., Del Carlo, M., Fratini, E., Escarpa, A., Compagnone, D., 2019. Microchim. Acta 186, 363.
Salminen, K., Grönroos, P., Eskola, J., Nieminen, E., Härmä, H., Kulmala, S., 2018. Electrochim. Acta 282, 147–154.
Scordo, G., Moscone, D., Palleschi, G., Arduini, F., 2018. Sens. Actuat. B. 258, 1015–1021.
Shamagsumova, R.V., Shurpik, D.N., Padnya, P.L., Stoikov, I.I., Evtugyn, G.A., 2015. Talanta 144, 559–568.
Shu, J., Qiu, Z., Zhou, Q., Tang, D., 2019a. Chem. Comm. 55, 3262–3265.
Shu, H., Jin, M., Tao, Y., 2019b. Graphene-based silicon modulators. Frontiers Inf. Technol. Electronic Eng. 20, 458–471. https://doi.org/10.1631/FITEE.1800407.
Silva, T.A., Fatibello-Filho, O., 2017. Anal. Methods 9, 4680–4687.
Smolko, V., Shurpik, D., Evtugyn, V., Stoikov, I., Evtugyn, G., 2016. Electroanal 28, 1391–1400.
Snowden, M.E., King, P.H., Covington, J.A., Macpherson, J.V., Unwin, P.R., 2010. Anal. Chem. 82, 3124–3131.
Sukumaran, P., Veettil, V.T., Rajappa, S., Li, C.Z., Alwarappan, S., 2017. Sens. Actuat. B. 247, 556–563.
Suprun, E.V., Arduini, F., Moscone, D., Palleschi, G., Shumyantseva, V.V., Archakov, A.I., 2012. Electroanal 24, 1923–1931.
Svegl, I.G., Bele, M., Ogorevc, B., 2008. Anal. Chim. Acta 628, 173–180.
Talarico, D., Arduini, F., Constantino, A., Del Carlo, M., Compagnone, D., Moscone, D., Palleschi, G., 2015a. Electrochem. Commun. 60, 78–82.
Talarico, D., Arduini, F., Amine, A., Moscone, D., Palleschi, G., 2015b. Talanta 141, 267–272.
Talarico, D., Cinti, S., Arduini, F., Amine, A., Moscone, D., Palleschi, G., 2015c. Environ. Sci. Technol. 49, 7934–7939.
Talarico, D., Arduini, F., Amine, A., Cacciotti, I., Moscone, D., Palleschi, G., 2016. Anal. Bioanal. Chem. 408, 7299–7309.
Thamilselvan, A., Rajagopal, V., Suryanarayanan, V., 2019. J. Alloy. Compd 786, 698–706.
Valappil, O.M., Alwarappan, S., Narayanan, T.N., 2015. Curr. Org. Chem. 12, 1163–1175.
Vicentini, F.C., Ravanini, A.E., Figueiredo-Filho, L.C., Iniesta, J., Banks, C.E., Fatibello-Filho, O., 2015. Electrochim. Acta 157, 125–133.
Vicentini, F.C., Raymundo-Pereira, P.A., Janegitz, B.C., Machado, S.A., Fatibello-Filho, O., 2016. Sensor. Actuat. B. 227, 610–618.
Vineesh, T.V., Alwarappan, S., Narayanan, T.N., 2015. Nanoscale 7, 6504–6509.
Wong, C.H.A., Ambrosi, A., Pumera, M., 2012. Nanoscale 4, 4972–4977.
Wong, A., Santos, A.M., Fatibello-Filho, O., 2018a. Sensor. Actuat. B. 255, 2264–2273.
Wong, A., Santos, A.M., Silva, T.A., Fatibello-Filho, O., 2018b. Talanta 183, 329–338.
Wong, A., Santos, A.M., Fava, E.L., Fatibello-Filho, O., Sotomayor, M.D.P.T., 2019. Microchem. J. 147, 365–373.
Yammouri, G., Mandli, J., Mohammadi, H., Amine, A., 2017. J. Electroanal. Chem. 806, 75–81.
Yammouri, G., Mohammadi, H., Amine, A., 2019. Chemistry Africa 2, 291–300.
Yang, H., Qiu, Y., Guo, X., 2017. Electrochim. Acta 235, 409–421.
Zakharova, E.A., Elesova, E.E., Noskova, G.N., Lu, M., Compton, R.G., 2012. Electroanal 24, 2061–2069.
Zeng, R., Luo, Z., Zhang, L., Tang, D., 2018. Anal. Chem. 90, 12299–12306.
Zeng, R., Luo, Z., Su, L., Zhang, L., Tang, D., Niessner, R., Knopp, D., 2019. Anal. Chem. 91, 2447–2454.
Zhang, X., Cao, Y., Yu, S., Yang, F., Xi, P., 2013. Biosens. Bioelectron. 44, 183–190.
Zhou, Q., Lin, Y., Zhang, K., Li, M., Tang, D., 2018. Biosens. Bioelectron. 101, 146–152.
Ławrywianiec, M., Smajdor, J., Paczosa-Bator, B., Piech, R., 2017. Food Anal. Method. 10, 3825–3835.